Theory of the Rotational and Vibrational Excitations in Solid Parahydrogen, and Frequency Analysis of the Infrared and Raman Spectra*

J. VAN KRANENDONK, G. KARL†
Department of Physics, University of Toronto, Toronto, Canada

The effects of the isotropic, anisotropic, and vibrational intermolecular forces on the rotation–vibration energy levels in solid parahydrogen are investigated theoretically. The main part of the shift of the rotation–vibration levels is due to the stretching of the molecules by the isotropic intermolecular forces. These shifts are calculated using a vibrating-rotor model for the hydrogen molecule, containing four anharmonicity constants determined from the spectroscopic data on gaseous hydrogen. The next most important interaction is the quadrupole–quadrupole interaction. For the matrix elements of the quadrupole moment between the rotation–vibration states we take the theoretical values calculated by Karl and Poll for an isolated molecule. On this basis a satisfactory account can be given of the shifts and splittings of all the zero-phonon features in the infrared and Raman spectra of solid parahydrogen and of ortho–para mixtures at low orthohydrogen concentrations. Of particular interest is the verification of the predicted shifts of the $S_1(0)$ and $S_2(0)$ lines, arising from the imperfect localization of the $J=2$ excitation on the vibrating molecule in the upper states of these transitions, and of the self-energy shifts of the rotational states due to the interaction with the lattice vibrations. The fine structure of the $S_1(0)$ line at low ortho concentrations, and the splitting of the $S_1(0)+S_1(0)$ doublet in the overtone infrared spectrum can also be understood using the unperturbed quadrupole moments and taking into account the imperfect localization of the rotational excitations. The complete frequency analysis yields empirical values of the vibrational coupling constant ($\epsilon'=0.49$ cm^{-1}) and the crystalline field constants ($\epsilon_{2c}=-0.03$ cm^{-1}, $\epsilon_{4c}=-2.60$ cm^{-1}), and leads to predictions concerning the frequency of the $S_0(0)$ infrared line, the splitting of the $S_1(0)$ Raman triplet and the position of the as yet unobserved third component, and the frequency of the $Q_1(0)+Q_1(1)$ line. For the remaining three unknown interaction parameters, six relations are derived of which the consistency is discussed in relation to the available experimental data.

1. INTRODUCTION

The rotational and vibrational motions of the molecules in solid hydrogen, and their infrared and Raman activity, have been investigated extensively in recent years, both experimentally[1–4] and theoretically.[5–9] The infrared activity in solid hydrogen is due to the dipole moments induced in pairs of neighboring molecules by the intermolecular forces, and is analogous to the pressure-induced infrared activity of hydrogen observed in the gaseous state.[10,11] The spectra of the solid are characterized by the appearance of a number of sharp zero-phonon lines and more extended zero-phonon bands, which are accompanied by broad and relatively intense phonon branches. These phonon branches arise from the strong dependence of the induced dipole moments on the intermolecular separations. The observed zero-phonon absorption features, together with the rotational and vibrational Raman spectra, which contain no phonon branches, have yielded detailed information about the shifts and splittings of the rotational and vibrational energy levels in solid hydrogen. The spectra of solid HD and D_2 are very similar, but the available experimental data are not as accurate and complete as for H_2, and we shall restrict ourselves to H_2.

The work described in this paper is aimed at investigating in how far it is possible to account for the observed energy levels in terms of the known properties of the isolated molecules and the known nature of the intermolecular forces, to an accuracy of a few tenths of a wave number, or about one part in 10^4. The number of unknown parameters characterizing the strength of the various parts of the intermolecular interaction in solid hydrogen relevant to this analysis is less than the number of available independent experimental data. A successful analysis of the data is therefore an indication of the adequacy of the theoretical model used to calculate the effect of the intermolecular forces on the rotational and vibrational levels of the

* This work was supported by a grant from the National Research Council of Canada.
† Present address: Department of Theoretical Physics, Oxford University, Oxford, England.
[1] H. P. Gush, W. F. J. Hare, E. J. Allin, and H. L. Welsh, Can. J. Phys. **38**, 176 (1960).
[2] H. P. Gush, J. Phys. Radium **22**, 149 (1961).
[3] S. S. Bhatnagar, E. J. Allin, and H. L. Welsh, Can. J. Phys. **40**, 9 (1962).
[4] V. Soots, E. J. Allin, and H. L. Welsh, Can. J. Phys. **43**, 1985 (1965).
[5] J. Van Kranendonk, Physica **25**, 1080 (1959).
[6] J. Van Kranendonk, Can. J. Phys. **38**, 240 (1960).
[7] H. P. Gush and J. Van Kranendonk, Can. J. Phys. **40**, 1461 (1962).
[8] V. F. Sears and J. Van Kranendonk, Can. J. Phys. **42**, 980 (1964).
[9] J. Van Kranendonk and V. F. Sears, Can. J. Phys. **44**, 313 (1966).
[10] D. A. Chisholm and H. L. Welsh, Can. J. Phys. **32**, 291 (1954).
[11] W. F. J. Hare and H. L. Welsh, Can. J. Phys. **36**, 88 (1958).

molecules in the solid. As is shown, such an analysis can be carried out for solid parahydrogen, to the accuracy stated, by taking into account all relevant intermolecular forces of the electrostatic and van der Waals types. On the next level of accuracy, of a few hundredths of a wave number, a host of additional interactions of the nonadiabatic and magnetic types come into play. A general analysis to this accuracy appears to be completely out of reach, and the discussion of effects of the order of 10^{-2} cm^{-1} must therefore be limited to specific features.

Of particular interest is the fact that the rotational motion of the molecules in the solid is free in the sense that the quantum number $J=\sum_i J_i$, where J_i is the rotational quantum number of molecule i, is a good quantum number also in the solid. This free rotation is an "inertial" free rotation and is quite different from the free rotation observed in many molecular crystals at sufficiently high temperatures, which is a "relaxation" type of free rotation. The "inertial" free rotation is characteristic of the molecules H_2, HD, and D_2, and persists down to absolute zero. Because of the small moment of inertia of the molecules, the anisotropic intermolecular interaction in the solid is so weak relative to the spacing of the rotational levels that states corresponding to different values of J are not mixed appreciably. Thus, in the ground state of solid parahydrogen all the molecules are in the state $J=0$. In the first excited rotational state one of the N molecules in the crystal is in the state $J=2$, and this level is $5N$-fold degenerate. This degeneracy is removed by the anisotropic intermolecular interaction (mainly the quadrupole–quadrupole interaction), and the $J=2$ level is spread out into a band of levels about 20 cm^{-1} wide, whereas the separation between the $J=2$ and $J=0$ levels is 356 cm^{-1}. The states in this $J=2$ band correspond to traveling rotational excitations which we shall call rotational excitons, or rotons for brevity. The dynamics and the infrared and Raman activity of these excitations have been discussed previously.[5,6]

The rotons introduced here are not analogous to magnons, or spin waves, but rather to the quantized vortices, or rotons, which can exist in liquid helium. A magnon in a ferromagnetic system of spins of magnitude $\frac{1}{2}$, say, is a traveling spin deviation, or spin reversal. In the presence of one magnon there is one spin with $S_z=-\frac{1}{2}$ rather than $S_z=+\frac{1}{2}$, a different spin at different times, but the magnitude of the angular momentum of each spin is equal to $\frac{1}{2}$ at all times. In the presence of one $J=2$ roton in solid parahydrogen, on the other hand, there is one molecule in the $J=2$ rather than in the $J=0$ state, a different molecule at different times, and only the magnitude of the total angular momentum of all the molecules in the crystal is constant. Such a roton is analogous to a roton in liquid helium to the extent that in both cases the total angular momentum is located at different points in the system at different times. The similarity of the two types of roton can be seen more clearly when solid parahydrogen is regarded as a liquid of hydrogen atoms in which strong correlations are present corresponding to the existence of hydrogen molecules located at lattice points.

The internal vibrational motion exhibits similar collective dynamical properties. In the ground state of the crystal, all the molecules are in the ground vibrational state corresponding to $v=0$. In the first excited vibrational state one of the N molecules is in the state $v=1$ and this state is N-fold degenerate (assuming that $J=0$). The intermolecular forces do not appreciably mix states corresponding to different values of $v=\sum_i v_i$, and v is a good quantum number also in the solid. The purity of v, in contrast to that of J, is a common property of most molecular crystal, since the intramolecular forces are in general large compared with the intermolecular forces. The part of the interaction between two neighboring molecules, which depends on the internuclear separations in both molecules, produces a coupling between the vibrational motions in the two molecules. This coupling removes the degeneracy of the $v=1$ level in the crystal and produces a $v=1$ band. In solid hydrogen this $v=1$ band is about 4 cm^{-1} wide, whereas the separation between the $v=1$ and $v=0$ levels amounts to 4153 cm^{-1}. The states in the $v=1$ band correspond to traveling vibrational excitations which are called vibrational excitons, or vibrons, for brevity. In the language of second quantization the vibrons are spinless particles, whereas the rotons are particles with spin 2. All these "particles" are, of course, bosons.

Apart from electronic excitations, which are not considered, three different types of excitation can thus exist in solid H_2, HD, and D_2: phonons, rotons, and vibrons. The interaction between these various excitons gives rise to a number of interesting scattering and bound-state problems some of which have been discussed previously.[6–9] Since the interaction is known in detail, in contrast to, e.g., that between an electron and an impurity in a metal, the study of the rotons and vibrons in solid hydrogen provides a most useful test for solid-state scattering theories. This lends a special interest to the investigation of the infrared and Raman spectra of solid hydrogen and its isotopes. Thermal excitation of the rotons and vibrons is impossible because of the high excitation energies involved, and even the phonons can be excited only weakly by thermal means since the melting temperature (14°K in H_2) is an order of magnitude smaller than the Debye temperature (100°K in H_2).

The main effect of the intermolecular forces on the molecules in the solid is a slight stretching of the internuclear axes of the molecules. Because of the rotation–vibration coupling and the anharmonicity of the intramolecular potential, this stretching causes a rather complicated shift of the rotation–vibration levels of the molecules. To account for these shifts, a dynamical model of the hydrogen molecule must be constructed

(Sec. 2). In Sec. 3 we discuss the nature of the anisotropic and vibrational intermolecular interaction responsible for the shift and splitting of the rotation–vibration levels in the solid. The effects of the isotropic intermolecular forces are calculated in Sec. 4. In Secs. 5, 6, and 7 we discuss in detail the pure rotational, the pure vibrational, and the mixed rotation–vibration excitations, and in Sec. 8, the overtone and double vibrational transitions are discussed. In Sec. 9, a frequency analysis is given of all the zero-phonon features in the infrared and Raman spectra of solid parahydrogen and of ortho–para mixtures at very low ortho-hydrogen concentrations. Finally, in Sec. 10, the results are summarized and the consistency of the model underlying the calculations is discussed.

2. DYNAMICAL MODEL OF THE H_2 MOLECULE

The energy levels of the free H_2 molecule have been determined experimentally from the Raman,[12] infrared,[13,14] and ultraviolet[15] spectra of gaseous hydrogen. We are interested here only in the rotation–vibration levels belonging to the ground electronic state. In the adiabatic approximation these levels are obtained by considering the motion of the nuclei in a potential $U(r)$ provided by the electrons and the Coulomb interaction between the nuclei. This model contains only the nuclear degrees of freedom and is called the vibrating-rotor model.[16,17] The most accurate calculation of the potential $U(r)$ from first principles is that of Kolos and Wolniewicz.[18] The calculation of the vibrational levels for this potential has been carried out by Poll and Karl[19] who have also calculated the contribution to the energies of the nonadiabatic effects. For the lower vibrational levels the energies calculated using the adiabatic approximation differ from the observed levels by about 1 cm^{-1}, and this is also the order of magnitude of the nonadiabatic effects. Thus, even for the relatively fast vibrational motion in H_2 it is a good approximation (1 part in 4000) to treat the motion of the electrons adiabatically, at least as far as the calculation of the energy levels is concerned.

We do not use the Kolos and Wolniewicz potential, but we determine an empirical potential by fitting the energies of a number of selected levels, calculated on the basis of the vibrating-rotor model, to the corresponding observed values. For the lower vibrational levels it is possible to construct in this way a model which reproduces the observed levels to an accuracy of better than 0.1 cm^{-1}. Since the nonadiabatic effects are of the order of 1 cm^{-1}, the resulting potential should be regarded as an effective one and not as the true potential defined for clamped nuclei. Strictly speaking, the dynamical response of the real molecules to external forces will therefore not be given entirely correctly by the model. However, in our applications, this difference is expected to be an order of magnitude smaller than the accuracy of 0.1 cm^{-1} we are aiming at and hence immaterial. The energies involved are of the order of 1000 cm^{-1}. In the solid, the shifts induced in the levels by the intermolecular forces are of the order of 10 cm^{-1}, or 1% of the total energy involved. The contribution of the nonadiabatic effects to the shifts can therefore be expected to amount to about 1% of the nonadiabatic contribution to the total energy, or about 10^{-2} cm^{-1}. Hence we may assume that our model does not only reproduce correctly the energy levels of the free molecule but also the shifts induced in the levels in the solid, at least within the accuracy of 0.1 cm^{-1}.

To obtain analytic expressions for the energy levels of the rotor in terms of the parameters characterizing the model, it is necessary to assume a simple expression for the potential $U(r)$. Since we are interested only in the first few vibrational states ($v=0, 1, 2$), it is most convenient to use the Dunham model,[20] in which the potential is expanded around its minimum at $r=r_e$ in powers of $r-r_e$. In terms of the dimensionless variable

$$x=(r-r_e)/r_e, \tag{1}$$

this expansion can be written in the form

$$U(r)=hca_0x^2(1+a_1x+a_2x^2+\cdots). \tag{2}$$

The potential (2) contains the parameters r_e and a_0, defining the harmonic potential, and the dimensionless anharmonicity constants a_1, a_2, $\cdots$. For a given value of the rotational angular momentum, J, the total potential appearing in the radial Schrödinger equation is given by

$$V(r)=U(r)+hcB_eJ(J+1)(1+x)^{-2}, \tag{3}$$

where

$$B_e=(\hbar/4\pi mcr_e^2), \tag{4}$$

m being the reduced mass of the rotor. The amplitude of vibration is small compared with the equilibrium distance r_e, i.e., we have $\langle x^2\rangle \ll 1$, where x is given by (1), and we may therefore expand the second term in Eq. (3) in powers of x. To see more clearly the nature of this expansion and of the approximation method based on it, we introduce the length l defined as

$$l=(\hbar/2\pi mc\omega_e)^{1/2}, \tag{5}$$

where $c\omega_e$ is the classical frequency of vibration (in

[12] B. P. Stoicheff, Can. J. Phys. **35**, 730 (1957).
[13] G. Herzberg, Can. J. Phys. **28**, 144 (1950).
[14] U. Fink, T. A. Wiggins, and D. H. Rank, J. Mol. Spectry. **18**, 384 (1965); J. V. Foltz, D. H. Rank, and T. A. Wiggins, *ibid.* **21**, 203 (1966).
[15] G. Herzberg and L. L. Howe, Can. J. Phys. **37**, 636 (1959).
[16] G. Herzberg, *Spectra of Diatomic Molecules* (D. Van Nostrand Co., Inc., New York, 1950).
[17] C. H. Townes and A. L. Schawlow, *Microwave Spectroscopy* (McGraw-Hill Book Co., New York, 1955).
[18] W. Kolos and L. Wolniewicz, J. Chem. Phys. **41**, 3663 (1964); **43**, 2429 (1965).
[19] J. D. Poll and G. Karl, Can. J. Phys. **44**, 1467 (1966).
[20] J. L. Dunham, Phys. Rev. **41**, 721 (1932).

TABLE I. Spectroscopic constants of the H_2 molecule (in cm^{-1}).

λ^n	Y_{lm}	Experimental values[a]	Calculated values[b] $n=0$	$n=2$	$n=4$
1	Y_{10}	4401.21	(4401.21)	(4401.21)	(4401.21
λ^2	Y_{20}	−121.34	0	(−121.34)	(−121.34)
λ^2	Y_{01}	60.853	0	(60.853)	(60.853)
λ^4	Y_{11}	−3.062	0	0	(−3.062)
λ^4	Y_{30}	0.813	0	0	(0.813)
λ^6	Y_{21}	5.8×10^{-2}	0	0	(5.8×10^{-2})
λ^6	Y_{02}	-4.67×10^{-2}	0	0	-4.65×10^{-2}
λ^8	Y_{31}	5.1×10^{-3}	0	0	(5.1×10^{-3})
λ^8	Y_{12}	1.8×10^{-3}	0	0	1.8×10^{-3}
λ^{10}	Y_{03}	5×10^{-5}	0	0	5×10^{-5}
λ^{10}	Y_{22}	-1.4×10^{-5}	0	0	-2×10^{-5}

[a] The experimental values are from Rank *et al.*,[14] except for Y_{22} which is from Herzberg and Howe.[15]
[b] The values in parentheses are fitted to the experimental values.

sec^{-1}) in the potential (2) for infinitesimal amplitudes,

$$\omega_e=(\hbar a_0/\pi m c r_e)^{1/2}. \tag{6}$$

The amplitude of vibration in the low vibrational states is of order l, and the range of the dimensionless variable

$$\xi=(r-r_e)/l=x/\lambda, \tag{7}$$

where

$$\lambda=l/r_e \tag{8}$$

is therefore of order unity. Introducing (6) and (7) into (3) and expanding the last term in Eq. (3) in powers of x, we get

$$V(r)/hc=\omega_e(\tfrac{1}{2}\xi^2+\lambda_1\xi^3+\lambda_2\xi^4+\cdots)+B_eJ(J+1)$$
$$+B_eJ(J+1)(-2\lambda\xi+3\lambda^2\xi^2-4\lambda^3\xi^3+\cdots), \tag{9}$$

where λ_n is defined as

$$\lambda_n=\tfrac{1}{2}\lambda^n a_n. \tag{10}$$

The expansion of the rotation–vibration interaction represented by the last term in Eq. (9) is an expansion in terms of the parameter λ. One should therefore regard λ as a small parameter which is imagined to vary from zero to its actual value (0.17 in H_2). One could consider a rotor with a fixed value of B_e, i.e., with constant m and r_e, and a varying amplitude l of vibration, i.e., varying λ. However, the quantities ω_e, B_e, and λ are not independent but are connected by the relation

$$B_e=\tfrac{1}{2}\lambda^2\omega_e, \tag{11}$$

which follows from Eqs. (4), (5), and (8). Regarding B_e as fixed therefore implies that ω_e is of order λ^{-2}. This is inconvenient, since we want to regard the last term in Eq. (9) as the perturbation and the first two terms as belonging to the unperturbed Hamiltonian which would then be of order λ^{-2}. It is therefore better to consider ω_e as fixed, λ as varying, and B_e as given by Eq. (11). It is true that the second unperturbed term in Eq. (9) is then of order λ^2, but this dependence of the unperturbed Hamiltonian on λ is harmless since this term is independent of ξ, so that it has no effect on the wave functions, and its effect on the energy levels can be taken into account exactly. We therefore adopt as the final expression for the potential energy

$$V(r)/hc=\omega_e(\tfrac{1}{2}\xi^2+\lambda_1\xi^3+\lambda_2\xi^4+\cdots)+\tfrac{1}{2}\lambda^2\omega_eJ(J+1)$$
$$+\tfrac{1}{2}\lambda^2\omega_eJ(J+1)(-2\lambda\xi+3\lambda^2\xi^2+\cdots), \tag{12}$$

where λ is regarded as a small parameter.

Two expansions are involved in the expression (12) for the potential: the Dunham expansion involving the anharmonicity constants λ_n and the expansion of the rotation–vibration interaction in powers of λ. In principle these two expansions are not related and may show different degrees of convergence. However, for the H_2 molecule, the constants a_n in Eq. (2) are of order unity, and according to Eq. (10) this means that the coefficients λ_n are of order λ^n. Using this fact we can make a systematic expansion of all quantities of interest in powers of λ.

Dunham has shown,[20] using the WKB method, that the energy levels, $E_{vJ}=hcF_{vJ}$, of a vibrating rotor can be expressed in the form

$$F_{vJ}=\sum_{l,m}Y_{lm}(v+\tfrac{1}{2})^lJ^m(J+1)^m, \tag{13}$$

where the spectroscopic constants Y_{lm} are definite expressions involving the parameters ω_e, λ, a_1, a_2, $\cdots$ characterizing the potential (12), which have been derived by Dunham in the form of power series in λ (actually in λ^4). The leading terms in the expressions for the seven most important constants are given by

$$\begin{aligned}
&Y_{10}=\omega_e[1+\tfrac{1}{16}\lambda^4A_{10}(a_1,\cdots,a_4)],\\
&Y_{20}=-\tfrac{3}{4}\lambda^2\omega_eA_{20}(a_1,a_2),\\
&Y_{01}=\tfrac{1}{2}\lambda^2\omega_e,\\
&Y_{11}=\tfrac{3}{2}\lambda^4\omega_eA_{11}(a_1),\\
&Y_{30}=\tfrac{1}{8}\lambda^4\omega A_{30}(a_1,\cdots,a_4),\\
&Y_{02}=-\tfrac{1}{2}\lambda^6\omega_e,\\
&Y_{21}=\tfrac{3}{4}\lambda^6\omega_eA_{21}(a_1,a_2,a_3).
\end{aligned} \tag{14}$$

The quantities A_{lm} are polynomials in the a_n, which are given by Dunham.[17,20] Empirical values of the constants Y_{lm} can be obtained by fitting the observed energy levels to the expression (13), and empirical values of the molecular constants ω_e, λ, a_1, a_2, $\cdots$ can then be obtained by solving Eqs. (14). Unfortunately, this procedure is not entirely unambiguous and has a limited range of applicability. In the first place, if one tries to include all the pure vibrational states ($J=0$), the expansion (13) does not converge, and one finds that the values of the Y_{l0} depend on the number of levels and terms one includes in the expansion.[15] This is clearly due to the fact that Eq. (13) is based on an expansion of the potential around the equilibrium position, and this expansion converges only for small displacements and not for the large displacements involved in the higher vibrational states. The representation of the levels by the formula (13) is therefore useful only for the lower vibrational states. For these states it is possible to arrive at a definite set of empirical constants Y_{lm}. The most accurate values are perhaps those derived recently by Rank *et al.*,[14] which are reproduced in Table I and which are used in this paper. These values agree closely with those obtained earlier by Stoicheff,[12] and by Herzberg and Howe.[15] In Table I the Y_{lm}'s are arranged in order of magnitude, and from the first column it is evident that this agrees with an ordering according to powers of λ. This agreement confirms the fact expressed by Eq. (10), that the anharmonicity constants λ_n in H_2 are of order λ^n.

A second ambiguity arises in the determination of the molecular constants ω_e, λ, a_1, a_2, $\cdots$ from the empirical values of the Y_{lm} using the Dunham formulas (14). This determination must also be carried out in steps corresponding to increasingly higher powers of λ. We will include terms of order $n=4$, but to illustrate the procedure, we also discuss the cases $n=0$ and $n=2$. For $n=0$, the set (14) reduces to the single equation $Y_{10}=\omega_e$. In this approximation we thus have $\omega_e=Y_{10}$ and $\lambda=0$. The constants a_n remain undetermined, but this is irrelevant since $\lambda=0$. For $n=2$, the set (14) reduces to the three equations

$$\begin{aligned} Y_{10}&=\omega_e,\\ Y_{20}&=-\tfrac{3}{4}\lambda^2\omega_e A_{20}(a_1, a_2),\\ Y_{01}&=\tfrac{1}{2}\lambda^2\omega_e, \end{aligned} \tag{15}$$

TABLE II. Molecular constants of the H_2 molecule (ω_e in cm^{-1}).

	$n=0$	$n=2$	$n=4$
ω_e	4401.21	4401.21	4402.84
λ	0	0.1663	0.1663
a_1	$\cdots$	−1.607	−1.607
a_2	$\cdots$	1.898	1.898
a_3	$\cdots$	$\cdots$	−2.060
a_4	$\cdots$	$\cdots$	1.965
a_5	$\cdots$	$\cdots$	0.11

in the three unknowns ω_e, λ, A_{20}. Hence a_1 and a_2 cannot be determined separately in this approximation, only the combination A_{20}. The value of A_{20} turns out to be the same for $n=2$ and $n=4$, and one may therefore assume that a_1 and a_2 for $n=2$ have the same values as for $n=4$, and this is done in the column $n=2$ in Table II. Although much better than the $n=0$ model, it is clear that for our purpose (0.1 cm^{-1}) the $n=2$ model is not adequate. For $n=4$, we get the five equations

$$\begin{aligned} Y_{10}&=\omega_e[1+\tfrac{1}{16}\lambda^4 A_{10}(a_1, \cdots, a_4)]\\ Y_{20}&=-\tfrac{3}{4}\lambda^2\omega_e A_{20}(a_1, a_2),\\ Y_{01}&=\tfrac{1}{2}\lambda^2\omega_e,\\ Y_{11}&=\tfrac{3}{2}\lambda^4\omega_e A_{11}(a_1),\\ Y_{30}&=\tfrac{1}{8}\lambda^4\omega_e A_{30}(a_1, \cdots, a_4) \end{aligned} \tag{16}$$

in the six unknowns ω_e, λ, A_{10}, A_{20}, A_{11}, A_{30}, or ω_e, λ, a_1, $\cdots$, a_4. We now need one more relation to get a definite set of values of the molecular parameters, but all relations of order λ^4 have been used. The only way to proceed is to use one of the relations of order λ^6. This is slightly inconsistent, since we have already neglected terms of order λ^6 in the expressions for Y_{20} and Y_{11} in the Eqs. (16), but this procedure leads nonetheless to a practical model. There are two relations of order λ^6, viz., the last two in Eq. (14). From Y_{02}, in conjunction with Y_{01}, one can obtain directly a value of λ. However, it is much more convenient to use Y_{21} and to determine λ from Y_{10} and Y_{01}, in a way to be explained presently, which also leads to a more accurate value of λ. We therefore add the last relation in (14) to (16). To solve the resulting six equations in the six unknowns ω_e, λ, a_1, $\cdots$, a_4, we write the first equation in (14) in the form

$$\omega_e=Y_{10}[1-\tfrac{1}{16}\lambda^4 A_{10}(a_1, \cdots, a_4)]. \tag{17}$$

The lowest nonvanishing terms in the remaining equations are then given by

$$\begin{aligned} Y_{20}/Y_{10}&=-\tfrac{3}{4}\lambda^2 A_{20}(a_1, a_2),\\ Y_{01}/Y_{10}&=\tfrac{1}{2}\lambda^2,\\ Y_{11}/Y_{10}&=\tfrac{3}{2}\lambda^4 A_{11}(a_1),\\ Y_{30}/Y_{10}&=\tfrac{1}{8}\lambda^4 A_{30}(a_1, \cdots, a_4),\\ Y_{21}/Y_{10}&=\tfrac{3}{4}\lambda^6 A_{21}(a_1, a_2, a_3). \end{aligned} \tag{18}$$

From these equations, one can easily obtain the constants λ, a_1, $\cdots$, a_4 in terms of the spectroscopic constants appearing in the left-hand members, and ω_e can then be calculated from Eq. (17). The resulting values of the molecular constants agree closely with those obtained by Rank *et al.*[14] and are shown in the last column of Table II. To test the consistency of the model, one can calculate some of the remaining constants Y_{lm} from Eqs. (14) using the molecular constants

TABLE III. Frequencies of a number of transitions in the free H_2 molecule calculated using the $n=4$ model, and the corresponding experimental values.

Line	Observed[a] frequency in cm^{-1}	Calculated frequency in cm^{-1}
$S_0(0)$	354.4	354.4
$S_0(1)$	587.0	586.9
$Q_1(0)$	4161.2	4161.2
$Q_1(1)$	4155.3	4155.3
$S_1(0)$	4497.8	4497.8
$S_1(1)$	4712.9	4712.4
$Q_2(0)$	···	8087.0
$Q_2(1)$	8075.4	8075.5
$S_2(0)$	8406.4	8406.8
$S_2(1)$	8604.3	8604.6

[a] From Refs. 12, 13, and 14.

given in Table II. The values calculated in this way are shown in the last column of Table I by the numbers not enclosed in parentheses. Of particular interest is the fact that the calculated value of Y_{02} agrees within the limits of accuracy with the experimental value. This agreement makes possible the procedure outlined above of adding one $n=6$ relation to Eqs. (16) which are of order $n=4$. We remark that the constant Y_{31} contains a_5, and hence Y_{31} can not be calculated in the $n=4$ model. It is, of course, possible to use the experimental value of Y_{31} to obtain a value of a_5 (which is equal to $a_5=0.11$), but this value is not very reliable because it is quite sensitive to the small corrections which have to be applied to the molecular constants given in Table II when terms of order λ^8, i.e., of the same order as Y_{31}, are taken into account in the right-hand members of Eqs. (16).

When one constructs the next approximation corresponding to $n=6$, by taking into account all terms of order λ^6, one obtains eight equations of the type (14) in the eight unknowns ω_e, λ, a_1, ···, a_6. In principle this yields a unique set of values for these constants, but in practice one runs into the difficulty that no experimental value can be obtained for Y_{40} in spite of the fact that all the pure vibrational levels have been observed.[15] This situation can presumably not be improved by making more accurate measurements, and is rather to be interpreted as an indication that for the H_2 molecule the Dunham model ceases to be useful for $n>4$. Thus, the approximation corresponding to $n=4$ appears to be a natural limit of the model, at least for the H_2 molecule, and it is fortunate that this gives an accuracy adequate for our purpose.

In summary, the model we use for the H_2 molecule is a vibrating rotor with an effective potential given by Eq. (12) and characterized by the constants ω_e, λ, a_1, ···, a_4 given in the last column of Table II. The energy levels of the rotor are calculated by including in the Dunham formula (13) the first seven spectroscopic constants Y_{lm} listed in Table I. The frequencies of a number of transitions calculated on the basis of this model are given in Table III together with the available experimental values.

3. THE ANISOTROPIC AND VIBRATIONAL INTERMOLECULAR INTERACTION IN SOLID HYDROGEN

We must now investigate how the rotation–vibration levels of the molecules discussed in the preceding section are affected by the intermolecular forces operative in the solid. We ignore the lattice vibrations for the time being and we assume that the centers of mass of the molecules are arranged on the sites of a rigid hcp lattice which is the crystal structure of solid parahydrogen.[21] The interaction between two molecules, 1 and 2, in the solid can be decomposed in the form

$$V_{12}=c_{12}+f_1(r_1)+f_1(r_2)+f_2(r_1,r_2)+g(\omega_1)+g(\omega_2)+g'(r_1;\omega_1)+g'(r_2;\omega_2)+a_0(\omega_1,\omega_2)+a_1(r_1;\omega_1,\omega_2)+a_1(r_2;\omega_2,\omega_1)+a_2(r_1,r_2;\omega_1,\omega_2). \quad (19)$$

The orientation of the internuclear axis of molecule i in a frame whose z axis is the intermolecular axis, $\mathbf{R}_{12}$, is denoted by $\omega_i\equiv(\theta_i,\phi_i)$, and the orientation in a frame which is the same for all the molecules, e.g., with the z axis along the hexagonal axis of the crystal, will be denoted by Ω_i. All the quantities in Eq. (19) are, of course, also functions of R_{12}, but this dependence will usually not be indicated explicitly. The term c_{12} in Eq. (19) is independent of r_i and ω_i, and is defined as

$$c_{12}=\langle V_{12}(r_e,r_e;\omega_1,\omega_2)\rangle, \quad (20)$$

where r_e is the equilibrium value of r_i in the free molecule, and the sharp brackets indicate an unweighted average over all values of ω_1 and ω_2. The term $f_1(r_1)$ in Eq. (19) depends only on r_1 and is defined such that $f_1(r_e)=0$. The remaining terms in Eq. (19) are defined in a similar way and the complete set of defining equations is

$$f_1(r_e)=f_2(r_e,r_2)=f_2(r_1,r_e)=\langle g(\omega_1)\rangle=g'(r_e;\omega_1)=\langle g'(r_1;\omega_1)\rangle=\cdots=\langle a_2(r_1,r_2;\omega_1,\omega_2)\rangle=0. \quad (21)$$

It is easy to show that the decomposition (19) is determined uniquely by the Eqs. (20) and (21).

The total energy of interaction in the solid is equal to the sum of the pair potential (19) over all pairs of molecules,

$$V=\sum_{i<j}V_{ij}(r_i,r_j;\omega_i,\omega_j)=C+F_1+F_2+G+G'+A_0+A_1+A_2. \quad (22)$$

Corresponding terms in Eqs. (19) and (22) are denoted by small and capital letters, respectively. The term C is the total cohesive energy of the crystal and is of no

[21] J. Van Kranendonk and H. P. Gush, Phys. Letters **1**, 22 (1962).

interest in the present context. The term F_1 is given by

$$F_1=\sum_i \sum_{j\neq i} f_1(r_i; R_{ij}) \equiv \sum_i U_1(r_i), \qquad (23)$$

which is also the defining equation of the function $U_1(r)$. The interaction (23) changes the effective intramolecular potential of each molecule from the value $U(r)$, given by Eq. (2), characteristic of the free molecule, to $U(r)+U_1(r)$. The effect of the resulting slight stretching of the molecules on the rotation–vibration levels is discussed in Sec. 4. The term F_2 in Eq. (22) is defined as

$$F_2=\sum_{i<j} f_2(r_i, r_j; R_{ij}), \qquad (24)$$

and gives rise to a coupling between the vibrational motions in neighboring molecules. This coupling causes a broadening of the excited vibrational levels of the crystal into vibrational exciton bands, as explained in Sec. 1. The interaction (24) is mainly due to the dependence on the internuclear separations of the attractive van der Waals forces[5] and is essentially operative only between nearest-neighboring molecules. The coupling (24) has recently been discussed in detail by James and Van Kranendonk[22] in connection with the observed[4,23] anomaly in the intensity ratio of the vibrational Raman lines of ortho and para molecules in solid H_2 and D_2.

The term G in Eq. (22) is given by

$$G=\sum_i \sum_{j\neq i} g(\omega_i; \mathbf{R}_{ij}) \equiv \sum_i V_c(\mathbf{\Omega}_i), \qquad (25)$$

and this equation defines the function $V_c(\mathbf{\Omega})$, where $\mathbf{\Omega}$ denotes the orientation relative to the hexagonal axis of the crystal. The interaction (25) is of the crystalline field type in the sense that each term in Eq. (25) depends on the orientation of only one molecule, but no true crystalline field is involved. The interaction (25) is partly due to the anisotropic part of the van der Waals interaction which comes into play as a result of the blowing up of the crystal by the zero-point lattice vibrations and partly to the polarization, or self-energy, effects resulting from the coupling of the rotational motion of the molecules and the lattice vibrations, as discussed elsewhere.[9] The main effect of the interaction (25) is a splitting of the localized rotational states of the molecules in the solid. The term G' in Eq. (22) is also of the crystalline field type except that it acts also on the vibrational motion. It can be expected to be a factor of order $\lambda=0.17$ smaller than the term G and will therefore be neglected. The next term in Eq. (22), A_0, is given by

$$A_0=\sum_{i<j} a_0(\omega_i, \omega_j; \mathbf{R}_{ij}), \qquad (26)$$

and this interaction is responsible for the broadening of the rotational levels in the crystal into rotational exciton bands. The term A_0 is mainly due to the electrostatic quadrupole–quadrupole interaction between the molecules and has been discussed in previous papers.[5–7] Finally, the terms A_1 and A_2 are defined in a similar manner but are not very important and are not written down explicitly.

We now discuss briefly the role of the lattice vibrations in determining the rotation–vibration levels in the solid.[9] We are interested in temperatures (<4°K) which are very low compared with the Debye temperature ($\sim$100°K), and we may assume that the crystal is at absolute zero. First, in a nonrigid lattice, the potential energy introduced in Eqs. (19) and (22) is not equal to its value in the rigid lattice but rather to the expectation value of the instantaneous interaction over the zero-point lattice vibrations. However, this does not affect the nature of the decomposition defined by Eqs. (19), (20), and (21), and these equations are valid also for the nonrigid lattice. The magnitude of the interaction (22) in the solid is, of course, different for the rigid and nonrigid lattices. However, we do not calculate the magnitude of the various terms in Eq. (22) from the corresponding terms in the pair potential for isolated molecules, since this potential is not known sufficiently accurately, but we obtain instead empirical values for the coupling constants from an analysis of the observed infrared and Raman spectra of the solid. These constants therefore refer to the nonrigid lattice, but this need not be indicated explicitly in the notation. The only exception is the quadrupolar interaction for which we take the electrostatic interaction between the known quadrupole moments of the free molecules, calculated for a rigid lattice. The justification for this procedures rests on the fact that the quadrupolar interaction, ϕ_{12}, between two molecules situated at $\mathbf{R}_1$ and $\mathbf{R}_2$, is a potential function as far as its dependence on both $\mathbf{R}_1$ and $\mathbf{R}_2$ is concerned: $\Delta_1\phi_{12}=\Delta_2\phi_{12}=0$. When we expand ϕ_{12} in powers of the displacements $\mathbf{u}_1$ and $\mathbf{u}_2$ of the molecules from their equilibrium positions, it is clear that the linear terms vanish upon taking the expectation value over the ground state of the lattice. To estimate the contribution of the quadratic terms to the expectation value, we may assume in first approximation that the lattice vibrations are isotropic in the sense that $\langle u_{i\alpha}^2\rangle=u^2$ is independent of $\alpha=x, y, z$, and that the displacements of different molecules are uncorrelated, $\langle u_{i\alpha}u_{j\beta}\rangle=0$ if $i\neq j$. The contribution of the quadratic terms to $\langle\phi_{12}\rangle$ is then proportional to $(\Delta_1+\Delta_2)\phi_{12}$ and hence vanishes. Thus the effect of the zero-point lattice vibrations on the quadrupolar interaction is a higher-order effect depending on the anisotropy and correlations in the displacement distribution. We neglect these small effects and assume that the quadrupolar interaction is given by its value in the rigid lattice. The same argument applies to all the other multipole interactions. The effect of the lattice vibrations on the other interactions, such as the ani-

[22] H. M. James and J. Van Kranendonk, Phys. Rev. (to be published).

[23] A. H. M. Rosevaer, G. Whiting, and E. J. Allin, Can. J. Phys. (to be published).

sotropic dispersion interaction, $R^{-6}Y_{20}(\theta)$, is not small, as discussed in detail elsewhere,[9] and it is therefore important to realize that the coupling constants we obtain refer to the nonrigid lattice. Finally, we mention that the coupling between the lattice vibrations and the rotational motion of the molecules gives rise to polarization, or self-energy, effects[9] which produce shifts and splittings of the rotational levels which are discussed in subsequent sections. The corresponding effects due to the coupling of the internal vibrational motion of the molecules and the lattice vibrations are completely negligible because of the large difference between the internal vibrational frequency and the Debye frequency.

4. EFFECT OF THE STRETCHING OF THE MOLECULES IN THE SOLID ON THE ROTATION-VIBRATION LEVELS

The most important term in the expression (22) for the interaction energy in the solid, apart from the constant term C which does not affect the rotation–vibration levels, is the term F_1 defined by Eq. (23). This term does not give rise to a coupling between the molecules but to a change in the effective intramolecular potential of each molecule. Following the approximation scheme outlined in Sec. 2, we expand the change $\Delta U(r)=U_1(r)$ in the potential $U(r)$, due to the interaction (23), in powers of $r-r_e$. Writing this expansion in the form

$$\Delta U(r)=-hc\omega_e(\lambda\mu_1\xi+\lambda^2\mu_2\xi^2+\cdots), \tag{27}$$

where ξ is given by Eq. (7), one can easily see that the dimensionless constants μ_i characterizing the strength of the interaction should be regarded as being independent of λ. We retain only the first two terms in Eq. (27) and calculate the resulting changes in the molecular constants and energy levels up to terms of relative order of magnitude λ^2, i.e., we retain terms linear in μ_1, μ_1^2, and μ_2. However, it turns out that the terms containing μ_1^2 are insignificant, and we therefore give explicit expressions only for the terms linear in μ_1 and μ_2.

The intramolecular potential of a molecule in the solid is given by the sum of the potential (2) of the free molecule

$$U(r)=hc\omega_e(\tfrac{1}{2}\xi^2+\lambda_1\xi^3+\cdots+\lambda_4\xi^6) \tag{28}$$

and the perturbation (27), and is given by

$$U'(r)=hc\omega_e(\tfrac{1}{2}\xi^2+\lambda_1\xi^3+\cdots+\lambda_4\xi^6-\lambda\mu_1\xi-\lambda^2\mu_2\xi^2). \tag{29}$$

All quantities pertaining to the perturbed molecules are indicated by a prime. To find the energy levels of the rotor with the potential (29), we write Eq. (29) in the form of Eq. (28) by introducing a change of variables. The minimum of $U'(r)$ comes at $\xi=\xi_0$, where

$$\xi_0=(r_e'-r_e)/l=\lambda\mu_1, \tag{30}$$

and the new equilibrium internuclear distance is therefore given by

$$r_e'=r_e(1+\lambda^2\mu_1). \tag{31}$$

Since μ_1 turns out to be positive in solid hydrogen, the effect of the interaction (23) is to stretch the intramolecular bond of the molecules. With the new variable

$$\xi'=(l/l')(\xi-\xi_0)=(\omega_e'/\omega_e)(\xi-\xi_0), \tag{32}$$

we can write Eq. (29) in the desired form

$$U'(r)=hc\omega_e'(\tfrac{1}{2}\xi'^2+\lambda_1'\xi'^3+\cdots+\lambda_4'\xi'^6). \tag{33}$$

Introducing the new anharmonicity constants a_n' by the relation analogous to Eq. (10),

$$\lambda_n'=\tfrac{1}{2}\lambda'^n a_n', \tag{34}$$

we find that the changes, $\Delta\omega_e=\omega_e'-\omega_e$, etc., in the molecular constants listed in Table II, as far as the terms linear in μ_1 and μ_2 are concerned, are given by

$$\begin{aligned}\Delta\omega_e&=\lambda^2(\tfrac{3}{2}a_1\mu_1-\mu_2)\omega_e,\\ \Delta\lambda&=-\lambda^2[(1+\tfrac{3}{4}a_1)\mu_1-\tfrac{1}{2}\mu_2]\lambda,\\ \Delta a_n&=\lambda^2(a_{n1}\mu_1+a_{n2}\mu_2),\end{aligned} \tag{35}$$

where

$$\begin{aligned}a_n&=na_n-3a_1a_n+(n+3)a_{n+1},\\ a_{n2}&=2a_n.\end{aligned} \tag{36}$$

Because of the identical form of the old and new potentials (28) and (33), the energy levels of the perturbed rotor are given by the Dunham formula (13) with Y_{lm} replaced by Y_{lm}', where Y_{lm}' is the same function (14) of the new molecular constants ω_e', λ', a_1', $\cdots$, a_4' as Y_{lm} is of the unprimed constants. The resulting changes, $\Delta Y_{lm}=Y_{lm}'-Y_{lm}$, in the spectroscopic constants can be calculated from Eqs. (14) and (35), and the result can be written in the form

$$\Delta Y_{lm}=B_{lm}\mu_1+C_{lm}\mu_2. \tag{37}$$

The quantities B_{lm} and C_{lm} are of the order of magnitude $\lambda^2 Y_{lm}$ and are obtained in the form of power series in

TABLE IV. Numerical values in cm^{-1} of the coefficients B_{lm} and C_{lm}, in the expression $\Delta Y_{lm}=B_{lm}\mu_1+C_{lm}\mu_2$ for the change in the spectroscopic constants Y_{lm}.

lm	B_{lm}	C_{lm}
10	−293.3	−121.7
20	−4.48	−23.0
01	−3.37	0
11	−0.111	−0.533
30	+0.78	−0.77
21	0	0
02	0	0

λ^4. Retaining only the terms of order $\lambda^2 Y_{lm}$, we find

$$B_{10}=\tfrac{3}{2}\lambda^2 a_1 Y_{10},\ C=_{10}-\lambda^2 Y_{10}, \tag{38}$$

$$B_{20}=-2\lambda^2 Y_{20}-\tfrac{3}{2}\lambda^2(\tfrac{5}{2}a_1 a_{11}-a_{21})\,Y_{01},$$

$$C_{20}=-\tfrac{3}{2}\lambda^2(\tfrac{5}{2}a_1 a_{12}-a_{22})\,Y_{01}, \tag{39}$$

$$B_{01}=-2\lambda^2 Y_{01}, \qquad C_{01}=0, \tag{40}$$

$$B_{11}=-\lambda^2(4+\tfrac{3}{2}a_1)\,Y_{11}+3\lambda^4 a_{11}Y_{01},$$

$$C_{11}=\lambda^2 Y_{11}+3\lambda^4 a_{12}Y_{01}, \tag{41}$$

$$B_{30}=-\lambda^2(4+\tfrac{3}{2}a_1)\,Y_{30}+\tfrac{1}{4}\lambda^4 Y_{01}$$
$$\times[10a_{41}-35(a_1a_{31}+a_3a_{11})-17a_2a_{21}+(225/4)$$
$$\times(2a_1a_2a_{11}+a_1^2a_{21})-(705/8)a_1^3a_{11}], \tag{42}$$

$$C_{30}=\lambda^2 Y_{30}+\tfrac{1}{4}\lambda^4 Y_{01}[10a_{42}-35(a_1a_{32}+a_3a_{12})$$
$$-17a_2a_{22}+(225/4)(2a_1a_2a_{12}+a_1^2a_{22})-(705/8)a_1^3a_{12}],$$

$$B_{21}=C_{21}=B_{02}=C_{02}=0. \tag{43}$$

The numerical values of these coefficients, corresponding to the values of the spectroscopic and molecular constants given in the columns $n=4$ in Tables I and II, are shown in Table IV. Using these values and the Dunham formula (13), one can calculate the shifts in the energy levels of the molecules as functions of μ_1 and μ_2. The parameters μ_1 and μ_2 cannot be calculated sufficiently accurately from first principles, and we therefore regard μ_1 and μ_2 as adjustable parameters. The value of μ_1 was estimated in a previous paper[6] to be about 4×10^{-2}, and this can be expected to be the order of magnitude of μ_1. (Note that the definitions of μ_1 and μ_2 given here differ from the previous ones[6] by the factors λ and λ^2, respectively.) The shifts in the vibrational levels due to the interaction (23) are therefore of the order of 10 cm^{-1}. The determination of empirical values of μ_1 and μ_2 is discussed in Sec. 10.

5. THE PURE ROTATIONAL EXCITATIONS

Now, we consider the effect of the intermolecular interaction on the pure rotational states of the solid. In these states all the molecules are in the ground vibrational state $v=0$, and we restrict ourselves to the rotational states $J=0$, 1, and 2. Apart from the terms C and F_1, which were discussed in Sec. 4, the only terms in the expression (22) for the total interaction which have nonvanishing matrix elements within the manifold of the pure rotational states are the terms G and A_0 defined by Eqs. (25) and (26), respectively.

We consider first the effect of the crystalline field term G in the absence of the coupling term A_0 so that we may assume that the rotational excitations are completely localized. The function $V_c(\mathbf{\Omega})$, defined by Eq. (25), which is the energy of the central molecule in the total crystalline field, can be expanded in terms of the spherical harmonics $Y_{lm}(\mathbf{\Omega})$. Because of the homonuclear character of the central molecule, only the terms corresponding to even l appear, and since we are interested only in the states $J=0$, 1, 2, we need to consider only the terms $l=2$ and $l=4$. Finally, because of the point symmetry of the hcp structure, only the $m=0$ terms appear. The function $V_c(\mathbf{\Omega})$ can therefore be written in the form

$$V_c(\mathbf{\Omega})=\epsilon_{2c}(4\pi/5)^{1/2}Y_{20}(\mathbf{\Omega})+\epsilon_{4c}(4\pi/9)^{1/2}Y_{40}(\mathbf{\Omega}), \tag{44}$$

where ϵ_{2c} and ϵ_{4c} are constants. The origin of the $l=2$ term has been discussed in Ref. 9. It arises from the $l=2$ anisotropic van der Waals interaction between the molecules. In a lattice of the hcp structure, the sum of this interaction over the twelve neighbors vanishes. However, solid hydrogen is blown up considerably by the zero-point lattice vibrations, and, because of the anisotropy of the elastic properties of the crystal, one must expect that the blowing up is not perfectly isotropic. The result is a uniform deviation of the axis ratio (c/a) from the value $(8/3)^{1/2}$ characteristic of the hcp structure, and this leads to a nonvanishing value of ϵ_{2c}. A second contribution to ϵ_{2c} comes from the local distortion of the lattice resulting from the coupling between the rotational motion of the molecules and the lattice vibrations.[9] The two contributions to ϵ_{2c} are of the same order of magnitude but of opposite sign, so that the resulting value of ϵ_{2c} is very small. The term ϵ_{4c} in Eq. (44) arises from the $l=4$ anisotropic van der Waals forces. This term does not vanish when summed over the twelve neighbors in a hcp lattice, and the constant ϵ_{4c} can therefore be expected to be correspondingly larger than ϵ_{2c}. It is not possible at present to make reliable theoretical estimates of the values of ϵ_{2c} and ϵ_{4c}, and we therefore regard these constants as adjustable parameters to be determined from the experimental data.

The effect of the interaction (44) on the localized rotational states can easily be calculated. The eigenstates are clearly the states $|Jm\rangle$, where m refers to the hexagonal axis, and the eigenvalues of V_c are given by

$$E_c(Jm)=\sum_{l=2,4}\epsilon_{lc}C(JlJ;000)C(JlJ;m0m), \tag{45}$$

where the C's are Clebsch–Gordan coefficients. For $J=0$ we have $E_c(00)=0$, and for $J=2$ we get

$$E_c(2m)=-\tfrac{2}{7}c_m\epsilon_{2c}+\tfrac{1}{21}a_m\epsilon_{4c}, \tag{46}$$

where

$$a_{\pm2}=1, \qquad a_{\pm1}=-4, \qquad a_0=6,$$
$$c_{\pm2}=1, \qquad c_{\pm1}=-\tfrac{1}{2}, \qquad c_0=-1. \tag{47}$$

In addition to the splitting (45), which leaves the average energy unchanged, the rotational levels suffer a shift arising from the self-energy of the rotational states due to the coupling with the lattice vibrations. This effect has been discussed by Van Kranendonk

and Sears[9] and the resulting shift in the energy is given by

$$E_s(J) \equiv \tfrac{1}{5} \sum_m E_s(J, m) = -\epsilon_s \frac{7J(J+1)}{2(2J-1)(2J+3)}. \quad (48)$$

The constant ϵ_s has been estimated in Ref. 9 and is of the order of 1 cm^{-1} ($\epsilon_s = \frac{9}{7}\tilde{E}_\infty$ in the previous notation).

The coupling term A_0 defined by Eq. (26), is responsible for the hopping of the $J=2$ rotational excitations in solid parahydrogen. We first ignore the interaction (44), i.e., we consider free rotons. The interaction $a_0(\boldsymbol{\omega}_1, \boldsymbol{\omega}_2; \mathbf{R}_{12})$ between two molecules can be expanded in terms of products of spherical harmonics, $Y_{l_1 m_1}(\boldsymbol{\omega}_1) \times Y_{l_2 m_2}(\boldsymbol{\omega}_2)$. Within the subspace corresponding to the presence of one $J=2$ excitation in a crystal of pure parahydrogen, only the terms corresponding to $l_1=l_2=2$ have nonvanishing matrix elements. For the calculation of the $J=2$ band, the interaction a_0 may therefore be assumed to be given by

$$a_0(\boldsymbol{\omega}_1, \boldsymbol{\omega}_2; \mathbf{R}_{12}) = 4\pi\epsilon \sum_{m=-2}^{+2} c_m Y_{2m}(\boldsymbol{\omega}_1) Y_{2m}^*(\boldsymbol{\omega}_2). \quad (49)$$

Since $c_{-m}=c_m$, the coupling of the type $l_1=l_2=2$ is characterized by three independent parameters. A more significant characterization of the three types of interaction can be obtained by introducing the functions[5]

$$f_{j0}(\boldsymbol{\omega}_1, \boldsymbol{\omega}_2) = \sum_m C(22j; m, -m) Y_{2m}(\boldsymbol{\omega}_1) Y_{2-m}(\boldsymbol{\omega}_2), \quad (50)$$

which are eigenfunctions of $\mathbf{J}^2$ and J_z, where $\mathbf{J}=\mathbf{J}_1+\mathbf{J}_2$ is the total rotational angular momentum of the two molecules. Using Eq. (50), we can write Eq. (49) in the form

$$a_0 = 4\pi \sum_j \epsilon_j \alpha_j f_{j0}(\boldsymbol{\omega}_1, \boldsymbol{\omega}_2), \quad (51)$$

where the numerical constants $\alpha_0 = 5^{1/2}$, $\alpha_2 = \frac{1}{2}(7)^{1/2}$, $\alpha_4 = (70)^{1/2}$ have been introduced for convenience. The interaction a_0 is hence characterized by the three parameters ϵ_0, ϵ_2, and ϵ_4. The relation between the coefficients ϵc_m in Eq. (49) and ϵ_j in Eq. (51) is

$$\epsilon c_m = (-1)^m \sum_j \alpha_j C(22j; m, -m) \epsilon_j = \sum_j c_m(j) \epsilon_j, \quad (52)$$

where in the last member we have introduced the notation

$$c_m(j) = (-1)^m \alpha_j (22j; m, -m). \quad (53)$$

In virtue of our choice of the coefficients α_j, the coefficients (53) satisfy the relation $c_2(j)=1$. In general, one must expect that all three coefficients ϵ_j are different from zero. In solid hydrogen, the molecules are relatively far apart and the main contribution to the interaction (49) comes from the electrostatic quadrupole–quadrupole interaction. For this interaction only ϵ_4 is different from zero, and we get

$$a_0 = 4\pi\epsilon_4\alpha_4 f_{40}(\boldsymbol{\omega}_1, \boldsymbol{\omega}_2) = 4\pi\epsilon \sum_m a_m Y_{2m}(\boldsymbol{\omega}_1) Y_{2m}^*(\boldsymbol{\omega}_2), \quad (54)$$

where the coefficients $a_m = c_m(4)$ are given by (47), and

$$\epsilon = (Q_1 Q_2 / 5 R_{12}^5). \quad (55)$$

The fact that, for the quadrupole coupling, only the term in Eq. (51) corresponding to the maximum value of j appears is characteristic for multipole interactions. Thus, for $l_1=l_2=1$, there are two terms corresponding to $j=0$ and $j=2$, and the latter is the dipole–dipole interaction. Likewise, for $l_1=2$, $l_2=4$, the term corresponding to $j=6$ is the quadrupole–hexadecapole interaction,[7] etc. In the case of the $l_1=l_2=2$ interaction, the terms $j=0$ and $j=2$ arise from the higher-order anisotropic overlap and dispersion forces. We assume that at the nearest-neighbor separation in solid hydrogen these terms are negligible compared with the $j=4$ term and that this term is equal to the quadrupole–quadrupole interaction. We thus adopt for a_0 the expression

$$a_0(\boldsymbol{\omega}_1, \boldsymbol{\omega}_2; \mathbf{R}_{12}) = 4\pi\epsilon_{00}(a/R_{12})^5 \sum_m a_m Y_{2m}(\boldsymbol{\omega}_1) Y_{2m}^*(\boldsymbol{\omega}_2), \quad (56)$$

where the a_m are given by Eq. (47), and $a=3.75$ Å is the lattic constant.

The matrix element, $\langle vJ \mid Q(r) \mid v'J' \rangle$, of the quadrupole moment, $Q(r)$, of an isolated H_2 molecule between the radial rotation–vibration states, $\mid vJ \rangle$, have been calculated by Karl and Poll[24] using the function $Q(r)$ calculated by Kolos and Wolniewicz.[18] One can easily verify that the stretching of the molecules discussed in Sec. 4 has a negligible effect on the quadrupole matrix elements. It is, of course, possible that the quadrupole moment $Q(r)$ of a molecule in the solid, for a given value of r, is different from that of a free molecule as a result of the distortion of the electronic wave function by the intermolecular interaction. This effect has been investigated by one of us,[25] and it turns out to be quite small. We therefore assume that in the solid the quadrupole matrix elements have the same values as for the isolated molecule. For the $J=2$ band, the coupling constant ϵ_{00} in Eq. (56) is then given by

$$\epsilon_{00} = \langle 00 \mid Q \mid 02 \rangle^2 / 5a^5, \quad (57)$$

and for $a=3.75$ Å and $\langle 00 \mid Q \mid 02 \rangle = 0.4858$ a.u., this gives $\epsilon_{00} = 0.580$ cm^{-1}. This value is rather different from the value 0.50 cm^{-1} used previously,[5,6] but there is no doubt that the present value is the correct one. One of the aims of this paper is, in fact, to investigate whether it is possible to give a complete analysis of the observed infrared and Raman spectra by assuming

[24] G. Karl and J. D. Poll, J. Chem. Phys. **46**, 2944 (1967).
[25] G. Karl (to be published).

that the various quadrupolar coupling constants have the theoretical values.

The wave functions and energy eigenvalues of the states in the $J=2$ band in pure parahydrogen have been discussed previously.[5,6] The wave functions describing the motion of the $J=2$ excitation through the lattice are Bloch waves and are characterized by a wave vector $\mathbf{k}$. Since there are two molecules per unit cell in a hcp lattice, there are ten $J=2$ states for each value of $\mathbf{k}$. Because the wavelength of the exciting radiation in both infrared and Raman experiments is very large compared with the lattice constant, only the states with $\mathbf{k}=0$ are optically active. Of the ten $\mathbf{k}=0$ states, five are even and five are odd with respect to an inversion at a point midway between the two molecules in a unit cell.[6] The corresponding energy levels are given by

$$E_m^+(0)=0.903a_m\epsilon_{00}, \quad E_m^-(0)=4.20a_m\epsilon_{00}, \quad (58)$$

where the constants a_m are given by Eq. (47). The numerical factors in Eq. (58) are lattice sums which come in because the quadrupolar interaction between all pairs of molecules has been taken into account. The quantum number m in Eq. (58) is the component of $\mathbf{J}$ along the hexagonal axis. For $\mathbf{k}=0$, but not for $\mathbf{k}\neq 0$, the $J=2$ band eigenfunctions are therefore also eigenfunctions of the crystalline field interaction (44), and we can simply add the energy perturbations (44) and (46) to (58) to obtain the total energies of the $\mathbf{k}=0$ states due to the anisotropic forces.

The even $\mathbf{k}=0$ states are Raman active and give rise to the rotational $S_0(0)$ Raman triplet[3] shown in Fig. 1. The three components in the order of increasing Raman shift correspond to $m=\pm 1, \pm 2, 0$. This assignment follows from the fact that the main contribution to the splitting of the $S_0(0)$ level comes from the quadrupolar interaction. With the positive coupling constant (57) one gets the given order of the levels. The frequencies, in cm^{-1}, of the three Raman components will be denoted by $\nu_R[S_0(0)]_m$. Combining the results (37), (45), (46), and (58), we obtain the following expression for these frequencies[26]:

$$\nu_R[S_0(0)]_m=\nu_g[S_0(0)]-17.1\mu_1-1.3\mu_2 +a_m(0.903\epsilon_{00}+\tfrac{1}{21}\epsilon_{4c})-\tfrac{2}{7}c_m\epsilon_{2c}-\epsilon_s, \quad (59)$$

where $\nu_g[S_0(0)]$ is the frequency of the $S_0(0)$ transition in a free molecule, observed in the spectra of gaseous hydrogen, and the coefficients a_m and c_m are given by Eq. (47).

Of the five odd $\mathbf{k}=0$ levels only the level corresponding to $m=\pm 2$ is infrared active[6] as a result of the point symmetry of the lattice. For the frequency of the $S_0(0)$ infrared line in pure parahydrogen we therefore obtain the expression

$$\nu_{IR}[S_0(0)]=\nu_g[S_0(0)]-17.1\mu_1-1.3\mu_2 +4.20\epsilon_{00}+\tfrac{1}{21}\epsilon_{4c}-\tfrac{2}{7}\epsilon_{2c}-\epsilon_s. \quad (60)$$

The coefficient of μ_2 in Eqs. (59) and (60) is equal to $-68.3+67.0$ and is not known more accurately than to two significant figures. The discussion of the formulas (59) and (60) is continued in Sec. 9.

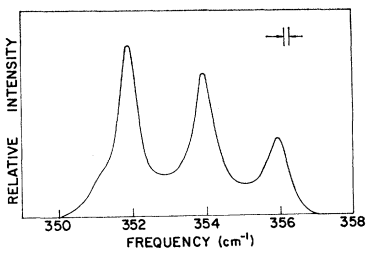

FIG. 1. The $S_0(0)$ line in the rotational Raman spectrum of solid parahydrogen observed by Bhatnagar, Allin, and Welsh (Ref. 3). The three components in the order of increasing frequency correspond to transitions to the even $m=\pm 1, \pm 2, 0$ sublevels of the $\mathbf{k}=0$ state in the $J=2$ rotational band, where m refers to the hexagonal axis. The fact that the $S_0(0)$ Raman line is split into a triplet rather than a doublet confirms that the crystal structure of solid parahydrogen is hcp rather than fcc.

6. THE PURE VIBRATIONAL EXCITATIONS

We now consider the manifold of states of a crystal of pure parahydrogen corresponding to the presence of one vibrational excitation

$$(v\equiv\sum_{i=1}^{N}v_i=1)$$

and no rotational excitations (all $J_i=0$). In the expression (22) for the total interaction energy only the term F_2, defined by Eq. (24), has nonvanishing matrix elements within this manifold of states, apart from the terms C and F_1 which were discussed in Sec. 4. The pair interaction $f_2(r_1, r_2)$ appearing in Eq. (24) is due to the dependence of the isotropic van der Waals interaction between the molecules 1 and 2 on r_1 and r_2, and is appreciable only for nearest-neighbor (nn) molecules. We expand $f_2(r_1, r_2)$ in powers of r_1-r_e and r_2-r_e and retain only the first nonvanishing term, which is

$$f_2(r_1, r_2)=-(\epsilon'/l^2)(r_1-r_e)(r_2-r_e), \quad (61)$$

where l is given by Eq. (5) and ϵ' is the vibrational coupling constant for nn molecules. The total vibrational interaction is

$$F_2=-(\epsilon'/l^2)\sum_{(i<j)}(r_i-r_e)(r_j-r_e), \quad (62)$$

where the sum extends over all nn pairs.

If $|1_i\rangle$ is the state of the crystal in which molecule i, at $\mathbf{R}_i$, is in the state $v=1$ and all the other molecules are in the state $v=0$, the stationary states in the pres-

[26] In Eq. (59) and in all further expressions for the frequencies of transitions we assume that the coupling constants ϵ_{00}, etc., are expressed in units cm^{-1}, i.e., a quantity ϵ in an expression for a frequency is actually ϵ/hc.

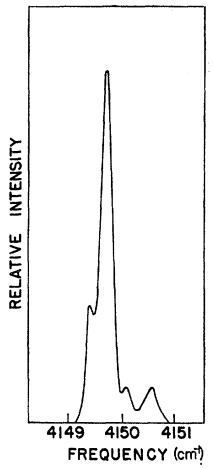

FIG. 2. The $Q_1(0)$ line in the vibrational Raman spectrum of solid parahydrogen observed by Soots, Allin, and Welsh (Ref. 4). The three weak components accompanying the main line are due to the hyperfine structure of the exciting mercury line used in the Raman experiment. The $Q_1(0)$ line is due to transitions to the even $\mathbf{k}=0$ level in the $v=1$ band.

ence of the coupling F_2 are given by

$$|\tau\rangle=\sum_{i=1}^{N} U_\tau(\mathbf{R}_i)|1_i\rangle. \tag{63}$$

$U_\tau(\mathbf{R}_i)$ is the amplitude, or wave function, describing the motion of the excitation through the lattice and satisfies the set of difference equations

$$-\tfrac{1}{2}\epsilon'\sum_{\mathbf{d}_i} U_\tau(\mathbf{R}_i+\mathbf{d}_i)=E_\tau U_\tau(\mathbf{R}_i), \tag{64}$$

where the sum extends over the vectors $\mathbf{d}_i$ connecting molecule i to its twelve neighbors. For a fcc lattice the solutions of Eq. (63) are the Bloch waves

$$U_{\mathbf{k}}(\mathbf{R}_i)=N^{-1/2}\exp(i\mathbf{k}\cdot\mathbf{R}_i), \tag{65}$$

and the corresponding energy eigenvalues are

$$E_{\mathbf{k}}=-\tfrac{1}{2}\epsilon'\sum_{\mathbf{d}}\cos(\mathbf{k}\cdot\mathbf{d}), \tag{66}$$

relative to the unperturbed energy of the $v=1$ state. For $\epsilon'>0$ these energies form a band extending from a minimum equal to $-6\epsilon'$ reached at $\mathbf{k}=0$ to a maximum equal to $+2\epsilon'$ assumed on a set of lines in $\mathbf{k}$ space. In an hcp lattice there are two molecules per unit cell, and the $v=1$ band consists of two overlapping subbands.[5] Nevertheless, as shown by James,[27] the over-all energy-level density is exactly the same in the two lattices and in fact in all close-packed lattices formed by stacking close-packed planes in arbitrary order.

In hcp parahydrogen the Raman active vibrational state is the even $\mathbf{k}=0$ state[8] which is shifted by the vibrational coupling by the amount $-6\epsilon'$. Combining this result with Eq. (37), we get the following expression for the frequency of the $Q_1(0)$ Raman line which is shown in Fig. 2:

$$\nu_{\mathrm{R}}[Q_1(0)]=\nu_i[Q_1(0)]-299.8\mu_1-170.8\mu_2-6\epsilon'. \tag{67}$$

The infrared $Q_1(0)$ line corresponds to transitions to the odd $\mathbf{k}=0$ state in the $v=1$ band. In pure parahydrogen this transition is not infrared active because of the point symmetry of the hcp lattice.[6] However, the $Q_1(0)$ line becomes infrared active in the presence of orthohydrogen impurities,[1] as shown in Fig. 3. At low ortho concentrations the $Q_1(0)$ line arises from transitions to the $v=1$ band of states in the host crystal accompanied by an orientational transition ($\Delta J=0$, $\Delta m\neq 0$) in one of the ortho molecules. The presence of the ortho impurities spoils the selection rule $\Delta\mathbf{k}=0$ and transitions are possible to all the states in the $v=1$ band. The part of the $Q_1(0)$ line due to single ortho molecules has a definite line profile which is characteristic of the parahydrogen host crystal and which has been worked out in Ref. 8 using some simplifying assumptions. The result is a line profile extending from $-6\epsilon'$ to about $1.2\epsilon'$ following a $\Delta\nu^{3/2}$ law, where $\Delta\nu$ is the frequency measured from the low frequency end of the line. When this profile is smeared out to take into account the finite resolving power used in the infrared absorption experiments, a profile peaked at about $0.6\epsilon'$ is obtained. Identifying the observed frequency with the peak of this profile, we obtain the following expression for the frequency of the component of the $Q_1(0)$ line due to the presence of single orthohydrogen impurities:

$$\nu_{\mathrm{IR}}[Q_1(0)]=\nu_g[Q_1(0)]-299.8\mu_1-170.8\mu_2+0.6\epsilon'. \tag{68}$$

The last term is somewhat uncertain and should be given an error margin of $\pm 0.2\epsilon'$.

Finally, we consider the $Q_1(1)$ line at very low ortho concentrations, which arises from $v=0\rightarrow v=1$ transitions in isolated orthohydrogen impurities in a parahydrogen matrix. These transitions are governed by the selection rule $\Delta m=\pm 2$, so that only the transitions $m=\pm 1\rightarrow m=\mp 1$ occur.[8] The splitting of the $J=1$ level into the two levels $m=0$, $m=\pm 1$, given by Eq. (45), therefore does not give rise to a shift or splitting of the $Q_1(1)$ line. The $v=1$ excitation on an ortho molecule in a

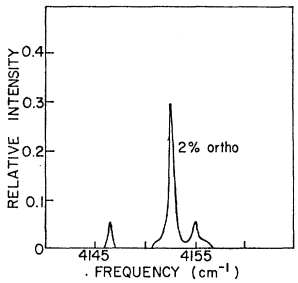

FIG. 3. The Q_1 branch in the infrared spectrum of solid hydrogen at a concentration of 2% orthohydrogen observed by Gush, Hare, Allin, and Welsh (Ref. 1). The low-frequency component is the $Q_1(1)$ line due to single orthohydrogen impurities. The main peak is the $Q_1(0)$ line due to the creation of a $v=1$ exciton of any wave vector in the parahydrogen host crystal, accompanied by an orientational transition in an isolated orthohydrogen impurity. The high-frequency component corresponds to the same $v=0\rightarrow v=1$ transition in the host crystal but accompanied by an orientational transition in a pair of neighboring ortho molecules. (See Ref. 8 for a detailed interpretation of the infrared Q branch.)

[27] H. M. James, Phys. Rev. **167**, 862 (1968).

para surroundings is not perfectly localized on the ortho molecule. The wave function $U_1(\mathbf{R}_i)$ of the vibrational impurity state is a solution of the equation

$$-\tfrac{1}{2}\epsilon' \sum_{\mathbf{d}_i} U(\mathbf{R}_i+\mathbf{d}_i) - W'\delta(\mathbf{R}_i;0)\,U_1(0) = E_1 U_1(\mathbf{R}_i), \tag{69}$$

where W' is the difference between the $v=1$, $J=0$ and $v=1$, $J=1$ states of a molecule in the solid in the absence of the vibrational coupling, which is given by

$$W' = W_g' + 0.2\mu_1 + 0.5\mu_2, \tag{70}$$

where $W_g' = \nu_g[Q_1(0)] - \nu_g[Q_1(1)] = 5.93$ cm^{-1} according to the measurements of Stoicheff.[12] The order of magnitude of μ_1 and μ_2 is $\mu_1 = 3\times10^{-2}$ and $\mu_2 = 0$ (cf. Sec. 10), and we therefore have that $W' = 5.94$ cm^{-1}. The energy E_1 of the localized state has been calculated previously[5] and in second order is given by

$$E_1 = -W'[1+3(\epsilon'/W')^2]. \tag{71}$$

Terms of higher order in (ϵ'/W') can most easily be calculated using the walk-counting method,[22] but these terms give no appreciable contribution to E_1. From Eqs. (37) and (71) we obtain the following expression for the frequency of the $Q_1(1)$ infrared line in the limit of very small ortho concentrations:

$$\nu_{IR}[Q_1(1)] = \nu_g[Q_1(1)] - 300.0\mu_1 - 171.3\mu_2 - 3(\epsilon'/W')\epsilon', \tag{72}$$

where $W' = 5.94$ cm^{-1}. Anticipating the result that ϵ' is of the order of 0.5 cm^{-1}, one may replace the last term by $-\frac{1}{4}\epsilon'$, since this term is only a very small correction. The expressions (67), (68), and (72) for the various vibrational frequencies are discussed further in Sec. 9.

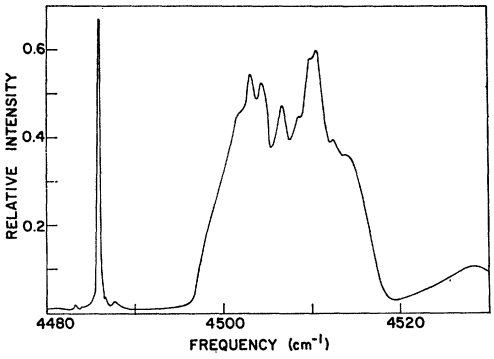

FIG. 4. The zero-phonon rotation–vibration band in the infrared spectrum of solid parahydrogen observed by Gush, Hare, Allin, and Welsh (Ref. 1). The broad absorption feature is the $Q_1(0)+S_0(0)$ combination band due to the creation of pairs of $v=1$ and $J=2$ excitations with arbitrary wave vectors $\mathbf{k}$ and $-\mathbf{k}$. The sharp feature is the $S_1(0)$ line which is due to transitions to the $m=\pm2$ sublevel of the $\mathbf{k}=0$ state in the band of the bound $v=1$, $J=2$ complexes. Because of the imperfect localization of the $J=2$ excitation on the $v=1$ molecule in the bound complexes, the frequency of the $S_1(0)$ line is lowered by 3.5 cm^{-1}, as discussed in the text in Sec. 7A.

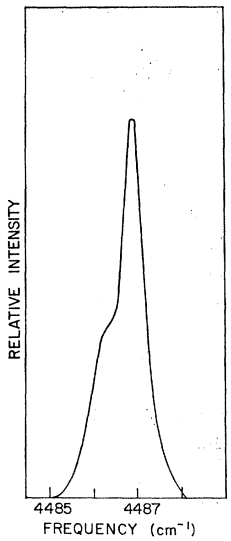

FIG. 5. The $S_1(0)$ line in the rotation–vibration Raman spectrum of solid parahydrogen observed by Soots, Allin, and Welsh (Ref. 4). Theoretically there should be three components corresponding in the order of increasing frequency to transitions to the sublevels $m=0$, ±2, ±1. As explained in the text in Sec. 9F, the main peak should be identified with the $m=\pm2$ component. The $m=0$ component is clearly visible, but the $m=\pm1$ component has not yet been resolved experimentally.

7. THE MIXED ROTATION-VIBRATION EXCITATIONS

In the manifold of states $\mathfrak{M}=\mathfrak{M}_1+\mathfrak{M}_2$ corresponding to the presence of one $v=1$ and one $J=2$ excitation in a crystal containing N parahydrogen molecules, there are $5N$ states in which the two excitations are on the same molecule (manifold $\mathfrak{M}_1$) and $5N(N-1)$ states in which they are on different molecules (manifold $\mathfrak{M}_2$). The state of the crystal in which the $v=1$ excitation is localized on molecule i, and the $J=2$, $J_z=m$ excitation on molecule j will be denoted by $|\,1_i;2_jm\rangle$, where z and m refer to the hexagonal axis of the crystal. Transitions from the ground state to the states $|\,1_i;2_im\rangle$ in $\mathfrak{M}_1$ give rise to the $S_1(0)-$, those to the states $|\,1_i;2_jm\rangle$, $i\neq j$, in $\mathfrak{M}_2$ to the $Q_1(0)+S_0(0)$ absorption feature (cf. Figs. 4 and 5). In the absence of the rotational and vibrational couplings, the states in $\mathfrak{M}_1$ and those in $\mathfrak{M}_2$ are degenerate, but are separated from each other by an energy W_1 which for free molecules[12] has the value 17.95 cm^{-1} and which in the solid is increased by the amount $0.6\mu_1+2.7\mu_2$, as follows from Eq. (37). The order of magnitude of this correction term is 0.02 cm^{-1}, and we therefore adopt for the rotation–vibration interaction in the solid the value $W_1=18.0$ cm^{-1}.

There are a number of ways in which the effects of the various interactions on the levels in the manifold $\mathfrak{M}$ can be calculated, depending on the order in which the interactions are introduced. If carried far enough, the different methods, if convergent, should lead to the same result. In the first method, one begins by neglecting the rotation–vibration interaction W_1, and one considers the manifolds $\mathfrak{M}_1$ and $\mathfrak{M}_2$ as degenerate. One introduces the quadrupolar interaction and the vibrational coupling as perturbations, and one obtains a rotation–vibration band consisting of a pure $J=2$ band overlapping a pure $v=1$ band. The over-all width of this band is clearly the sum of the widths of the $J=2$

and $v=1$ bands. One then introduces the interaction W_1, which gives rise to scattering processes of the roton and vibron and to the formation of bound complexes. This method is most convenient when one is interested in obtaining the scattering wave functions, but is less convenient when one wants to investigate the structure of the bound complexes. We are interested mainly in the latter, and we therefore follow the second method in which one begins with the manifolds $\mathfrak{M}_1$ and $\mathfrak{M}_2$ separated by the rotation–vibration interaction energy W_1. One first introduces the quadrupolar interaction, which transforms the states in $\mathfrak{M}_2$, $|\,1_i;\,2_jm\rangle$ $(i\neq j)$, into scattering states describing the scattering of a $J=2$ roton from a stationary $v=1$ excitation. The level density in the resulting band of states is exactly the same, in the limit of an infinitely large crystal, as that in the pure $J=2$ band, the difference being that the wave functions describe rotons undergoing scattering rather than free rotons. The quadrupolar interaction transforms the states in $\mathfrak{M}_1$, $|\,1_i;\,2_im\rangle$, into states in which the $J=2$ excitation is imperfectly localized on the stationary $v=1$ excitation. The resulting bound states are depressed in energy by this spreading of the $J=2$ wave function. A small splitting of the level also appears because the depression in energy is not exactly the same for the three sublevels $m=0,\ \pm1,\ \pm2$. However, the bound complexes do not move through the lattice under the action of the quadrupolar interaction, and the levels remain sharp. As the next perturbation, one introduces the vibrational coupling, the crystalline-field interaction, and the vibrational part of the quadrupolar interaction (to be defined in Sec. 7A below). These interactions are all of the same order of magnitude in their effect on the bound complexes and are an order of magnitude smaller than the quadrupolar interaction. They give rise to an additional splitting of the bound state levels and to a broadening of these levels, corresponding to the fact that the bound complexes are no longer immobile in the presence of these smaller perturbations.

The discussion of the splitting and broadening of the rotation–vibration levels, following the second method outlined above, is divided into four parts. In Sec. 7A we discuss the quadrupolar interaction and we extend the previously published calculations[5] by including third-order effects. In Sec. 7B, the vibrational coupling, the crystalline-field interactions, and the rotation–vibration coupling are discussed, and formulas for the frequencies of the $S_1(0)$ infrared and Raman lines are derived. In 7C, a sum rule for the double transitions $Q_1(0)+S_0(0)$ is used to obtain a formula for the mean frequency of this absorption band. Finally, in Sec. 7D, the fine structure of the $S_1(0)$ infrared line due to single orthohydrogen impurities is discussed.

A. Effect of the Quadrupole–Quadrupole Interaction on the Rotation–Vibration Levels

The largest interaction within the manifold of states $\mathfrak{M}$ is the quadrupolar interaction which, according to Eqs. (26) and (54), is given by

$$A=4\pi\sum_{i<j}(Q_iQ_j/5R_{ij}^5)\sum_m a_mY_{2m}(\omega_i)\,Y_{2m}{}^*(\omega_j), \quad (73)$$

where $Q_i=Q(r_i)$ is the instantaneous quadrupole moment of molecule i. The interaction (73) clearly contributes not only to the term A in Eq. (22) but also to the terms A_1 and A_2. We split the interaction A into a large and a small part by considering the matrix elements of A within the manifold $\mathfrak{M}$. The matrix elements of A within $\mathfrak{M}_1$ are given by

$$\langle 1_i;\,2_im\,|\,A\,|\,1_j;\,2_jn\rangle=\epsilon_{00}{}'(a/R_{ij})^5A_{mn}(\mathbf{\Omega}_{ij}), \qquad (i\neq j), \quad (74)$$

where

$$A_{mn}(\mathbf{\Omega})=(280\pi/9)^{1/2}(-1)^mC(224;\,m,\,-n)\,Y_{4,n-m}(\mathbf{\Omega}), \quad (75)$$

and $\mathbf{\Omega}_{ij}=(\theta_{ij},\,\phi_{ij})$ denotes the orientation of the intermolecular axis $\mathbf{R}_{ij}$ in a fixed frame with z axis along the hexagonal axis, and

$$\epsilon_{00}{}'=\langle 00\,|\,Q(r)\,|\,12\rangle^2/5a^5. \quad (76)$$

The matrix elements $\langle vJ\,|\,Q(r)\,|\,v'J'\rangle$ have been discussed in connection with Eq. (57). As for the notation of the coupling constants, the subscripts appearing in $\epsilon_{vv'}$, where

$$\epsilon_{vv'}=\langle v0\,|\,Q(r)\,|\,v2\rangle\langle v'0\,|\,Q(r)\,|\,v'2\rangle/5a^5, \quad (77)$$

denote the initial values of v and the prime in Eq. (76) indicates the appearance of the $v=0\rightarrow v=1$ off-diagonal elements. All the matrix elements involved in the coupling constants correspond to the $J=0\rightarrow J=2$ transition and the value of J therefore need not be indicated.

The matrix elements of A between the manifolds $\mathfrak{M}_1$ and $\mathfrak{M}_2$ are given by

$$\langle 1_i;\,2_im\,|\,A\,|\,1_i;\,2_jn\rangle=\epsilon_{01}(a/R_{ij})^5A_{mn}(\mathbf{\Omega}_{ij}), \qquad (i\neq j), \quad (78)$$

where

$$\epsilon_{01}=\langle 00\,|\,Q(r)\,|\,02\rangle\langle 10\,|\,Q(r)\,|\,12\rangle/5a^5. \quad (79)$$

Finally, the matrix elements within $\mathfrak{M}_2$ are of two types, those diagonal in v,

$$\langle 1_i;\,2_jm\,|\,A\,|\,1_i;\,2_kn\rangle=\epsilon_{00}(a/R_{jk})^5A_{mn}(\mathbf{\Omega}_{jk}) \qquad (i\neq j,\ i\neq k,\ j\neq k), \quad (80)$$

where ϵ_{00} is given by Eq. (57), and those off-diagonal in v,

$$\langle 1_i;\,2_jm\,|\,A\,|\,1_j;\,2_in\rangle=\epsilon_{11}{}'(a/R_{ij})^5A_{mn}(\mathbf{\Omega}_{ij}), \qquad (i\neq j) \quad (80')$$

where

$$\epsilon_{11}{}'=\langle 10\,|\,Q(r)\,|\,02\rangle^2/5a^5.$$

The matrix elements diagonal in v, Eqs. (78) and (80), are large, and the ones off-diagonal in v, Eqs. (74)

and (81), are small. As explained in connection with Eq. (57), we assume that the matrix elements $\langle vJ \mid Q(r) \mid v'J' \rangle$ for the molecules in the solid have the same values as for the free molecules. Using the values calculated by Karl and Poll,[14] and assuming $a=3.75$ Å, we get for the large coupling constants the values

$$\epsilon_{00}=0.580 \text{ cm}^{-1},$$

$$\epsilon_{01}=0.641 \text{ cm}^{-1},$$

whereas the small coupling constant (76) is equal to

$$\epsilon_{00}'=0.015 \text{ cm}^{-1}.$$

ϵ_{11}' has approximately the same value as ϵ_{00}', but the matrix elements involved in ϵ_{11}' have not been calculated.

The part of the interaction A, Eq. (73), defined by the large matrix elements (78) and (80), is discussed in this subsection and is called the quadrupolar interaction. We have included in the definition of the quadrupolar interaction the diagonal effects of the vibrational perturbation contained in the instantaneous interaction (73). These diagonal effects lead to the difference between the coupling constants ϵ_{00} and ϵ_{01} and make the quadrupolar interaction defined here different from that defined in Sec. 5 for the pure rotational states.

To calculate the effect of the quadrupolar interaction on the bound states in $\mathfrak{M}_1$, one can either employ perturbation theory or use the Green-function solution of the bound-state problem. The latter method was used previously[5] in combination with an expansion in powers of the interaction. The two methods lead to the same final result and we shall use here the perturbation method. First, we remark that the quadrupolar interaction, defined by Eqs. (78) and (80), leaves the $v=1$ excitations perfectly localized. Instead of the full set of $5N$ states in $\mathfrak{M}_1$ we therefore need to consider only the 5 states corresponding to the $v=1$ excitation being on a particular molecule. Second, one can easily show that because of the point symmetry of the hcp lattice, the correct states correspond to the values $m=0, \pm 1, \pm 2$ of the hexagonal axis. In second order the shift in the energy of the sublevel m is hence given by

$$\Delta E_m^{(2)}=-W_1^{-1}\sum_j \sum_n |\langle 1_i; 2_i m \mid A \mid 1_i; 2_j n\rangle|^2. \quad (81)$$

The sum over j extends over all the neighbors of molecule i, but we restrict this sum to the nearest neighbors only. This introduces a negligible error. Using Eqs. (78) and (75), expression (81) can be evaluated in a straightforward way, giving

$$\Delta E_m^{(2)}=-(D+\tfrac{3}{2}a_m)(\epsilon_{01}^2/W_1), \quad (82)$$

where $D=168$ and the constants a_m are given by Eq. (47). The second-order energy perturbation (81) arises from the hopping of the $J=2$ excitation from the vibrating molecule to a neighboring molecule and back. The hopping occurs between a $v=1$ and $v=0$ molecule, and the coupling constant appearing in Eq. (82) is therefore ϵ_{01}.

In third order the energy correction of the bound levels comes from a walk of three steps of the $J=2$ excitation beginning and ending on the vibrating molecule. The shift in the average energy of the five levels is given by

$$\Delta E^{(3)}=\tfrac{1}{5}\sum_m \Delta E_m^{(3)}=(1/5W_1^2)$$
$$\times\sum_{j,j'}\sum_{m,n,n'}\langle 1_i; 2_i m \mid A \mid 1_i; 2_j n\rangle\langle 1_i; 2_j n \mid A \mid 1_i; 2_{j'} n'\rangle$$
$$\times\langle 1_i; 2_{j'} n' \mid A \mid 1_i; 2_i m\rangle. \quad (83)$$

The contribution of each triangle of molecules i, j, j' is independent of the orientation of the triangle, since Eq. (83) involves a trace over all the projection quantum numbers. We restrict the sum in Eq. (83) to the 48 equilateral triangles with sides of length a. To calculate the contribution of one triangle, we choose the triangle to lie in the xz plane with $\mathbf{R}_{jj'}$ in the z direction. Equation (83) then reduces to

$$\Delta E^{(3)}=48(\epsilon_{01}^2\epsilon_{00}/W_1^2)(56\pi)(70)^{1/2}W(4242; 24)$$
$$\times\sum_m C(444; m, -m)|Y_{4m}(\Omega)|^2, \quad (84)$$

where W is a Racah coefficient and $\Omega=(60°, 0)$ denotes the orientation of $\mathbf{R}_{ij}$. The sum over m in Eq. (84) cannot be reduced further and must be calculated numerically. The result is

$$\Delta E^{(3)}=D'(\epsilon_{01}^2\epsilon_{00}/W_1^2), \quad (85)$$

where $D'=522.2$. The calculation of the third-order contribution to the splitting is much more complicated, but has been carried out completely numerically by Volterra.[28] The result can be written in the form

$$\Delta E_m^{(3)}-\Delta E^{(3)}=8.8a_m(\epsilon_{01}^2\epsilon_{00}/W_1^2). \quad (86)$$

The over-all splitting (86) amounts to about 0.05 cm^{-1} and is practically negligible for our purpose.

B. Vibration, Rotation–Vibrational, and Crystalline-Field Interactions

The pure vibrational coupling F_2, Eq. (62), has no matrix elements within the unperturbed manifold $\mathfrak{M}_1$. This means that the completely localized $S_1(0)$ excitations $\mid 1_i; 2_i m\rangle$ are not affected by the vibrational coupling. However, the imperfectly localized states resulting from the quadrupolar interaction, which to first order in (ϵ_{01}/W_1) are given by

$$\mid 1_i; 2_i m\rangle'=\mid 1_i; 2_i m\rangle - W_1^{-1}\sum_{j,n}\mid 1_i; 2_j n\rangle$$
$$\times\epsilon_{01}(a/R_{ij})^5 A_{nm}(\Omega_{ij}), \quad (87)$$

[28] V. Volterra (private communication). We are grateful to Dr. Volterra for communicating the results of his numerical calculations to us prior to publication.

are broadened by the vibrational coupling into a band corresponding to travelling $S_1(0)$ excitations. The matrix elements of the vibrational coupling between the states (87) corresponding to nearest-neighbor molecules ($R_{ij}=a$) are given by

$$'\langle 1_i;\, 2_i m \mid F_2 \mid 1_j;\, 2_j n\rangle' = (\epsilon'/W_1)\epsilon_{01}A_{mn}(\mathbf{\Omega}_{ij}). \quad (88)$$

A second contribution to the hopping elements $\mid 1_i;\, 2_i m\rangle \rightarrow \mid 1_j;\, 2_j n\rangle$ comes from the vibrational part of the quadrupolar interaction (73) and is given by Eq. (74). The correction to the $S_1(0)$ states represented by the second term in Eq. (87) gives no contribution to these matrix elements, as one can easily verify. The total hopping element for the $S_1(0)$ excitations can therefore be written in the form

$$'\langle 1_i;\, 2_i m \mid F_2+A \mid 1_j;\, 2_j n\rangle' = [(\epsilon'\epsilon_{01}/W_1\epsilon_{00})\Delta_{ij}+\epsilon_{00}'/\epsilon_{00}] \times \epsilon_{00}(a/R_{ij})^5 A_{mn}(\mathbf{\Omega}_{ij}), \quad (89)$$

where $\Delta_{ij}=1$ if i and j are nearest neighbors, and $\Delta_{ij}=0$ for all other pairs. The factor behind the first bracketed expression in Eq. (89) is identical with the hopping element for the pure $J=2$ band. The $S_1(0)$ level is therefore broadened into an $S_1(0)$ exciton band with an over-all width equal to a factor of order

$$(\epsilon'\epsilon_{01}/W_1\epsilon_{00})+\epsilon_{00}'/\epsilon_{00} = (3.0+2.6)\times 10^{-2} \quad (90)$$

times that of the pure $J=2$ band, giving a width of about 1 cm^{-1}. Of interest are the energies of the Raman and infrared active even and odd $\mathbf{k}=0$ levels in the $S_1(0)$ band, which according to Eq. (89) and the previous result for the $J=2$ band[5] are given by

$$E_m^{\pm}(0) = S_1^{\pm} a_m \epsilon_{00}, \quad (91)$$

$$S_1^{+} = 1.17(\epsilon'/W_1)(\epsilon_{01}/\epsilon_{00})+0.903(\epsilon_{00}'/\epsilon_{00}),$$

$$S_1^{-} = 3.33(\epsilon'/W_1)(\epsilon_{01}/\epsilon_{00})+4.20(\epsilon_{00}'/\epsilon_{00}). \quad (92)$$

The numerical factors in Eq. (92) are lattice sums of the quadrupolar interaction, the sums in the terms containing ϵ' and ϵ_{00}', respectively, corresponding to nearest neighbors and all neighbors.

We must finally add the splitting due to the crystalline field interaction V_c, given by Eq. (44). For the $\mathbf{k}=0$ levels, V_c is diagonal in the band states, and the energy corrections to the $\mathbf{k}=0$ levels are simply given by Eq. (45). Collecting all the results, Eqs. (37), (45), (82), (85), (86), and (91), we obtain the following expression for the frequencies of the components of the $S_1(0)$ Raman line:

$$\nu_R[S_1(0)]_m = \nu_g[S_1(0)]-317.5\mu_1-174.8\mu_2 - \tfrac{2}{7}c_m\epsilon_{2c}+\tfrac{1}{21}a_m\epsilon_{4c}-(D+\tfrac{3}{2}a_m)(\epsilon_{01}^2/W_1) + (D'+8.8a_m)(\epsilon_{01}^2/\epsilon_{00}/W_1^2)+S_1^{+}a_m\epsilon_{00}-\epsilon_s'. \quad (93)$$

The $S_1(0)$ infrared line corresponds to transitions to the $m=\pm 2$ sublevel, and the frequency of the $S_1(0)$ infrared line is therefore given by

$$\nu_{IR}[S_1(0)] = \nu_g[S_1(0)]-317.5\mu_1-174.8\mu_2 - \tfrac{2}{7}\epsilon_{2c}+\tfrac{1}{21}\epsilon_{4c}-(D+\tfrac{3}{2})(\epsilon_{01}^2/W_1)+(D'+8.8) \times(\epsilon_{01}^2\epsilon_{00}/W_1^2)+S_1^{-}\epsilon_{00}-\epsilon_s'. \quad (94)$$

In Eqs. (93) and (94), the quantity ϵ_s' is the self-energy of the rotational motion of the molecules in the $S_1(0)$ state arising from the coupling with the lattice vibrations. This self-energy ϵ_s' is not identical with the corresponding quantity ϵ_s of the $S_0(0)$ level discussed in Sec. 5 [cf. Eq. (48)]. The $S_1(0)$ level is sharp, apart from the small broadening due to the hopping elements (89), and in the expression for the self-energy the energy in the intermediate states is therefore only the phonon energy amounting on the average to about $\frac{1}{2}\hbar\omega_D = 35$ cm^{-1}. The factor $\frac{1}{2}$ arises because in the sum over all phonon modes the Rayleigh–Jeans factor k^2 is cancelled by a factor k^{-2} [cf. Eq. (84) in Ref. 9] resulting in an approximately equal weight for all modes. The $S_0(0)$ level, on the other hand, is spread out into a band about 20 cm^{-1} wide, and, in the expression for the self-energy, the energy denominator therefore varies appreciably even if the spread in phonon energies is neglected. One can easily show that the net result is an enhancement of the self-energy effect. It is difficult to estimate the difference between ϵ_s and ϵ_s', but an order of magnitude calculation indicates that ϵ_s may be twice as large as ϵ_s'.

C. Mean Frequency of the $S_1(0)$ and $Q_1(0)+S_0(0)$ Infrared Bands

Let us denote the states in the manifold $\mathfrak{M}$ by $\mid n\rangle$ and the ground state of the crystal by $\mid 0\rangle$. The total integrated absorption coefficient of the $S_1(0)$ and $Q_1(0)+S_0(0)$ infrared bands (shown in Fig. 4) is then given by

$$\tilde{\alpha} = \tilde{\kappa}\sum_n \mid\langle n \mid \mu \mid 0\rangle\mid^2, \quad (95)$$

where μ is the component in the direction of polarization of the sum of the dipole moments induced in all pairs of molecules by the intermolecular forces.[6] The integrated absorption coefficient $\tilde{\alpha}$ corresponds to the absorption coefficient $\tilde{A}(\nu)$ per wavelength rather than per unit path length and has the nature of a transition probability. Because of spectroscopic stability, the quantity $\tilde{\alpha}$ is independent of the vibrational and anisotropic interactions since these interactions mix only the states in $\mathfrak{M}$ and do not admix appreciable states from other configurations. We now show that the mean frequency of absorption, or the first moment of $\tilde{A}(\nu)$, is also invariant, at least to a very good approximation. The mean frequency is given by

$$hc\langle\nu\rangle = \tilde{\alpha}^{-1}\sum_n (E_n-E_0)\mid\langle n \mid \mu \mid 0\rangle\mid^2 = \tilde{\alpha}^{-1}\sum_n [\langle 0 \mid \mu H \mid n\rangle\langle n \mid \mu \mid 0\rangle - \langle 0 \mid \mu \mid n\rangle\langle n \mid \mu H \mid 0\rangle], \quad (96)$$

where H is the full Hamiltonian of the crystal and $H \mid n\rangle = E_n \mid n\rangle$.

The dipole moment μ is a function of the orientations and internuclear separations of the molecules and consists of a sum of terms, such as a term linear in the coordinates $r_i - r_e$, a term quadratic in $r_i - r_e$, a term depending on the orientations of single molecules, etc. One can easily see that it is possible to choose from μ those terms, adding to μ', say, such that μ' has matrix elements only between the ground state and the states in $\mathfrak{M}$ and such that $\langle 0 \mid \mu' \mid n\rangle$ is very nearly equal to $\langle 0 \mid \mu \mid n\rangle$ for all $\mid n\rangle$. Since the states $\mid n\rangle$ correspond to the presence of one $v=1$ and one $J=2$ excitation, μ' should contain the terms in μ linear in the coordinates $r_i - r_e$ and depending on the orientations of a single molecule. These terms have no matrix elements to other states than those in $\mathfrak{M}$. However, there are also terms in μ, such as the cubic terms in the coordinates, which have matrix elements to states in $\mathfrak{M}$ as well as to other states, and the same is true of certain terms containing higher-order spherical harmonics of the orientations. However, all these terms give only very small contributions to the matrix elements $\langle 0 \mid \mu \mid n\rangle$ and may be neglected. For practical purposes we may therefore replace μ in Eq. (96) by μ'. We can then perform the sum over n, giving

$$hc\langle \nu \rangle = \tilde{\alpha}^{-1} \langle 0 \mid \mu' [H, \mu']_- \mid 0 \rangle. \tag{97}$$

The important point is that μ' is again simply a function of the internuclear separations and orientations of the molecules. This is also true of the vibrational and anisotropic interaction terms contained in the Hamiltonian H, and this interaction, V, therefore commutes with μ', so that we have $[H, \mu']_- = [H_0, \mu']_-$, where $H = H_0 + V$. From this it follows immediately that $\langle \nu \rangle = \langle \nu \rangle_0$, where $\langle \nu \rangle_0$ is the mean frequency in the absence of the perturbing interactions. It is, of course, possible to perform the sum over n in Eq. (96) in a formal way by introducing the operator P which projects onto the manifold $\mathfrak{M}$. One then obtains the expression

$$hc\langle \nu \rangle = \tilde{\alpha}^{-1} \langle 0 \mid \mu [H, P\mu]_- \mid 0 \rangle. \tag{98}$$

However, one must now show that $P\mu$ commutes with V, and this leads to the same considerations as given above.

To use the sum rule $\langle \nu \rangle = \langle \nu \rangle_0$, we must calculate the mean unperturbed frequency $\langle \nu \rangle_0$ for which we need the unperturbed integrated absorption coefficients of the $S_1(0)$ and $Q_1(0) + S_0(0)$ lines. These quantities have been calculated previously,[6] and in the present notation the result is, assuming that the lines are due to the quadrupolar induction effect only,

$$\frac{\tilde{\alpha}_0[S_1(0)]}{\tilde{\alpha}_0[Q_1(0) + S_0(0)]} = \frac{5 S_1^2 \langle 00 \mid Q \mid 12\rangle^2 \langle 00 \mid \alpha \mid 00\rangle^2}{8 S_2 \langle 00 \mid Q \mid 02\rangle^2 \langle 00 \mid \alpha \mid 10\rangle^2}. \tag{99}$$

The lattice sums are equal to $S_1 = 0.701$ and $S_2 = 12.80$.

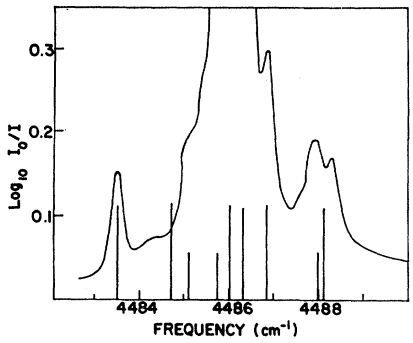

FIG. 6. The structure of the $S_1(0)$ infrared line at very low orthohydrogen concentrations, observed by Gush (Refs. 2 and 7). The satellite lines are due to transitions in the parahydrogen molecules on the nearest-neighbor sites of the orthohydrogen impurities. The 15-fold degenerate upper state in these transitions is split by the quadrupole–quadrupole interaction between the molecules. The splitting is considerably reduced by the fact that the $J=2$ excitation in the bound $v=1$, $J=2$ complex is imperfectly localized on the $v=1$ molecule (cf. Sec. 7D).

Using the values[24] $\langle 00 \mid Q \mid 12\rangle = 0.0784$, $\langle 00 \mid Q \mid 02\rangle = 0.4858$, and $\langle 00 \mid \alpha \mid 00\rangle = 5.46$ and $\langle 00 \mid \alpha \mid 10\rangle = 0.65$, all in atomic units, we find that the ratio (99) is equal to about 1/23. In the absence of the vibrational and anisotropic intermolecular forces, the $S_1(0)$ and $Q_1(0) + S_0(0)$ lines are sharp and their frequencies are given by

$$\nu_0[S_1(0)] = \nu_g[S_1(0)] - 317.5\mu_1 - 174.8\mu_2 - \epsilon_s',$$

$$\nu_0[Q_1(0) + S_0(0)] = \nu_g[Q_1(0)] + \nu_g[S_0(0)] - 316.9\mu_1 - 172.1\mu_2 - \epsilon_s. \tag{100}$$

In writing these expressions we have assumed that the frequency shifts ϵ_s and ϵ_s' due to the rotational self-energy are fixed and independent of the rotational coupling. This is clearly necessary, since the inclusion of the interaction with the lattice vibrations would spoil our sum rule. Using the result $\langle \nu \rangle = \langle \nu \rangle_0$, and assuming that the unperturbed intensity ratio (99) is equal to 1/23, we obtain from Eq. (100) the following result for the mean frequency for the $S_1(0)$ and $Q_1(0) + S_0(0)$ infrared absorption lines:

$$\langle \nu \rangle = \tfrac{1}{24}\nu_g[S_1(0)] + \tfrac{23}{24}\nu_g[Q_1(0) + S_0(0)] - 316.9\mu_1 - 172.2\mu_2 - \tfrac{23}{24}\epsilon_s - \tfrac{1}{24}\epsilon_s'. \tag{101}$$

There is an appreciable uncertainty involved in this expression because of the approximations made in the calculation of the ratio 1/23 of the unperturbed intensities.

D. Fine Structure of the $S_1(0)$ Line Due to Orthohydrogen Impurities

At low orthohydrogen concentrations the $S_1(0)$ infrared line shows a characteristic fine structure (cf. Fig. 6) which has been observed by Gush[2] and which has been interpreted[7] as due to the quadrupolar interaction between a para molecule in the $v=1$, $J=1$ upper stat

and a neighboring ortho molecule in the $v=0$, $J=1$ state. In Ref. 7, the $v=1$, $J=2$ state was assumed to be completely localized. The coupling constant of the quadrupolar interaction which splits the 25-fold degenerate state of the pair of molecules in the $v=1$, $J=2$ and $v=0$, $J=1$ states is then given by

$$\eta_{01}=\langle 01 \mid Q \mid 01\rangle\langle 12 \mid Q \mid 12\rangle/5a^5. \qquad (102)$$

In Ref. 7 this constant was denoted by ϵ and the small dependence of the quadrupole matrix elements on J was neglected. The best fit of the calculated to the observed fine structure was obtained by taking $\epsilon=0.52$ cm^{-1}. In this paper we attempt to account for the observed energy levels by assuming that the quadrupole matrix elements have the same values as for the free molecule. Using the theoretical values calculated by Karl and Poll,[24] we obtain for the coupling constant (102) the value $\eta_{01}=0.643$ cm^{-1}. When this value is used in the formulas derived in Ref. 7, a splitting is obtained which is much too large. The difficulty of obtaining a consistent set of quadrupolar coupling constants was noted in Ref. 7, and as a possible explanation the additional splitting of the rotational levels arising from the coupling to the lattice vibrations was suggested. This splitting is now known[9] to be too small to play a significant role in the fine structure of the $S_1(0)$ line. However, it is clear that the calculation in Ref. 7 is incomplete because the $J=2$ excitation in the $v=1$, $J=2$ bound state is assumed to be completely localized on the $v=1$ molecule, whereas it is actually spread out over the neighboring molecules because of the interaction with the $v=1$, $J'=2$ energy band states. The analytic calculation of the splitting of the 25-fold degenerate level of the spread out $v=1$, $J=2$ state and the $v=0$, $J=1$ state of the ortho molecule is very involved, but a numerical calculation has been carried out by Volterra.[28] Using for the coupling constant the value $\eta_{01}=0.643$ cm^{-1} and taking into account also the crystalline field interaction, Eq. (44), Volterra obtained a fine structure splitting which is in good agreement with the observed one. The observed fine structure of the $S_1(0)$ line can therefore be accounted for by using the quadrupolar coupling constants characteristic of the free molecules. It also follows that there is no clear cut evidence that the quadrupole–hexadecapole interaction gives an appreciable contribution to the splitting.

8. OVERTONE AND DOUBLE VIBRATIONAL TRANSITIONS

A. The $S_2(0)$ Transition

The manifold of states $\mathfrak{M}'$ corresponding to the presence of one $v=2$ and one $J=2$ excitation is entirely analogous to the manifold $\mathfrak{M}$ discussed in Sec. 7, the only difference being that the $v=1$ state is replaced by the $v=2$ state. We consider only the $S_2(0)$ infrared line arising from transitions to the $m=\pm 2$ component of the bound $v=2$, $J=2$ complex. For the frequency of this line we obtain the same formula as for the $S_1(0)$ line, Eq. (94), except for the following changes. The coefficients of μ_1 and μ_2 are different and can be obtained from Eq. (37). The quadrupolar constant appearing in the matrix element corresponding to the hopping of the $J=2$ excitation from the $v=2$ molecule to one of the neighboring $v=0$ molecules is ϵ_{02}, in the notation of Eq. (77), and the rotation–vibration interaction constant, W_2, has the value $W_2=35.1$ cm^{-1}. We neglect the term $S_2^-\epsilon_{00}$ arising from the hopping of the $v=2$, $J=2$ complex as a whole, since this term is only about half as great as for the $S_1(0)$ line. Collecting these results, we obtain the following expression for the frequency of the $S_2(0)$ infrared line:

$$\nu_{\mathrm{IR}}[S_2(0)]=\nu_g[S_2(0)]-619.9\mu_1-401.1\mu_2 -\tfrac{2}{7}\epsilon_{2c}+\tfrac{1}{21}\epsilon_{4c}-(D+\tfrac{3}{2})(\epsilon_{02}^2/W_2) +(D'+8.8)(\epsilon_{02}^2\epsilon_{00}/W_2^2)-\epsilon_s'. \qquad (103)$$

The $S_2(0)$ Raman line is very weak and has not been observed.

B. The $S_1(0)+S_1(0)$ Transition

We next consider the $S_1(0)+S_1(0)$ double transition in which in the upper state there are two $v=1$, $J=2$ complexes. In the infrared this transition gives rise to a sharp doublet which has been observed by Hare, Gush, and Welsh[29] and which is shown in Fig. 7. The main peaks lie at the frequencies 8971.0 cm^{-1} and 8973.1 cm^{-1}, so that the separation is $\Delta''=2.1$ cm^{-1}. It is evident from the observed absorption profile that there is some absorption in the region between the two main

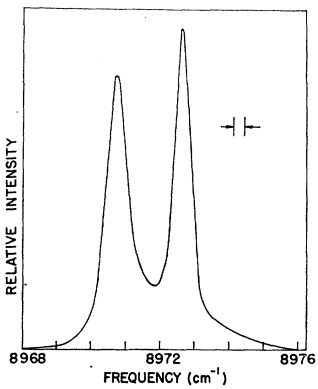

FIG. 7. The $S_1(0)+S_1(0)$ double transition in the infrared overtone spectrum of solid parahydrogen observed by Hare, Gush, and Welsh (Ref. 7). The 25-fold degenerate upper level in these transitions is split by the quadrupole–quadrupole interaction, but only two of the resulting levels are infrared active.

[29] H. P. Gush (private communication).

peaks and in the outer wings. The doublet has been interpreted[7] as arising from the splitting of the 25-fold degenerate upper state by the quadrupolar interaction. We here refine this calculation by taking into account the effect of the spreading of the $v=1$, $J=2$ states caused by the interaction with the $v=1$, $J'=2$ energy band states. We assume that the hopping of the $v=1$, $J=2$ complexes as a whole, which was discussed in Sec. 7B, may be neglected in this problem. Since the infrared activity is due to the dipole moments induced in pairs of molecules, which are appreciable only for nearest neighboring molecules, we may assume that in the upper state of the $S_1(0)+S_1(0)$ transition two nearest-neighboring molecules are in the $v=1$, $J=2$ state. In the absence of the quadrupolar interaction this level is 25-fold degenerate, and at an energy W_1 above this level there is a $10(N-2)$-fold degenerate level corresponding to one of the two $J=2$ excitations being on one of the $N-2$ molecules in the $v=0$ state. (At an energy $2W_1$ there is another level but this level may be ignored in the present context.) In the presence of the quadrupolar interaction the level at W_1 broadens into a band of the same width as the pure $J=2$ band. The states in this band describe the scattering of a $J=2$ roton by the complex consisting of the two neighboring molecules in the state $v_1=1$, $v_2=1$, $J_1+J_2=2$. This is an interesting scattering process involving the possibility that the incoming $J=2$ excitation is caught by the complex and the other $J=2$ excitation is emitted. However, we have not analyzed this process since the corresponding absorption band has not been observed.

To calculate the splitting of the bound $v_1=1$, $J_1=2$, $v_2=1$, $J_2=2$ complex we first introduce the quadrupolar interaction between the excited molecules 1 and 2, assuming perfectly localized $J=2$ excitations. The quadrupolar interaction with the surrounding molecules, which spreads out the $J=2$ excitations, is introduced afterwards. This procedure is correct if the relative energy separations of the levels are not changed too much by the second interaction. This condition appears to be satisfied, and we therefore expect that our calculation will give a reliable estimate of the effect of the spreading out of the $J=2$ excitations on the splitting. However, a detailed numerical analysis, including the effect of the crystalline field interaction, would be required to check the results.

The splitting due to the quadrupolar interaction between the molecules 1 and 2 was calculated in Ref. 7. Only two of the resulting levels are infrared active and the eigenstates and eigenvalues of these states are given by

$$|\pm\rangle=a_\pm\{|1,0\rangle-|0,1\rangle+\alpha_\pm(|2,-1\rangle-|-1,2\rangle)\}, \tag{104}$$

$$E_\pm=(10/49)[1\pm(55)^{1/2}]\eta_{11}, \tag{105}$$

where $\alpha_\pm=6^{1/2}[7\pm(55)^{1/2}]^{-1}$, $a_\pm$ is a normalization constant, and η_{11} is given by

$$\eta_{11}=\langle 12\,|\,Q\,|\,12\rangle^2/5a^5 \tag{106}$$

and has the value $\eta_{11}=0.714$ cm^{-1}. In Eq. (104) $|0,1\rangle$ is the state in which a $J=2$, $m=0$ excitation is on molecule 1 and a $J=2$, $m=1$ excitation on molecule 2, where m refers to the intermolecular axis pointing from 1 to 2. The two levels are each doubly degenerate and the remaining two states can be obtained from Eq. (104) by replacing all the quantum numbers m by $-m$.

We calculate the shift in the energy of the states $|\pm\rangle$ due to the quadrupolar interaction with the surrounding molecules in the same way as for a single $S_1(0)$ state, by means of the second-order perturbation formula

$$\Delta E_\pm=-\sum_n (E_n-E_\pm)^{-1}\,|\langle n\,|\,A\,|\,\pm\rangle|^2. \tag{107}$$

The sum extends over the $25\times2\times11=550$ intermediate states in which one of the $J=2$ excitations is on one of the two $v=1$ molecules and the other $J=2$ excitation is on one of the nearest-neighbor $v=0$ molecules. Expression (107) has been calculated numerically and for an $\alpha\alpha$ pair (the two $v=1$ molecules in the same hexagonal plane) the result is

$$\Delta E_+=-286.0\epsilon_{01}^2(W_1-1.71\eta_{11})^{-1},$$

$$\Delta E_-=-314.4\epsilon_{01}^2(W_1+1.31\eta_{11})^{-1}. \tag{108}$$

To see the physical significance of this result, we recall that the average second-order shift of a single $S_1(0)$ excitation is given by Eq. (82):

$$\Delta E^{(2)}=-168(\epsilon_{01}^2/W_1). \tag{109}$$

This energy shift is due to the occasional hopping of the $J=2$ excitation from the $v=1$ molecule to one of the twelve neighboring $v=0$, $J=0$ molecules. If one has two $S_1(0)$ excitations on neighboring molecules, each of the $J=2$ excitations can hop to one of the eleven neighboring $v=0$, $J=0$ molecules. One would therefore expect an average decrease in the energy by an amount given by Eq. (109) with the numerical constant $168=12\times14$ replaced by $2\times11\times14=308$. According to Eq. (108) the average shift is given by $300(\epsilon_{01}^2/W_1)$ in good agreement with this estimate. For an $\alpha\beta$ pair, the second-order corrections (107) are different, and the resulting levels turn out to lie between those of an $\alpha\alpha$ pair. These levels give rise to satellite components of the low frequency line of the $S_1(0)+S_1(0)$ doublet. When we identify the two main peaks as arising from transitions in $\alpha\alpha$ pairs, and when we neglect the effect of the crystalline field interaction (44), we obtain the following expressions for the frequencies of the $S_1(0)+$

$S_1(0)$ doublet:

$$\nu_{IR}[S_1(0)+S_1(0)]_+ = 2\{\nu_g[S_1(0)]-317.5\mu_1-174.8\mu_2-\epsilon_s'\} + (10/49)[1+(55)^{1/2}]\eta_{11}-286\epsilon_{01}^2(W_1-1.71\eta_{11}),$$

$$\nu_{IR}[S_1(0)+S_1(0)]_- = 2\{\nu_g[S_1(0)]-317.5\mu_1-174.8\mu_2-\epsilon_s'\} + (10/49)[1-(55)^{1/2}]\eta_{11}-314\epsilon_{01}^2(W_1+1.31\eta_{11}). \quad (110)$$

For the splitting,

$$\Delta''=\nu_{IR}[S_1(0)+S_1(0)]_+-\nu_{IR}[S_1(0)+S_1(0)]_-,$$

we obtain from Eq. (110) the value $\Delta''=2.0$ cm^{-1} in good agreement with the observed value (2.1 ± 0.1) cm^{-1}.

C. $Q_1(0)+Q_1(1)$ Transition

The $Q_1(0)+Q_1(1)$ transition corresponding to a simultaneous $\Delta v=1$, $\Delta J=0$ transition in an ortho-hydrogen molecule and a neighboring parahydrogen molecule has been observed in dilute solutions of ortho-hydrogen in parahydrogen. Apart from the fact that the ortho molecule makes a $v=1$ rather than a $v=0$ transition, the $Q_1(0)+Q_1(1)$ line is entirely analogous to the $Q_1(0)$ line discussed in Sec. 6. The shape of the $Q_1(0)+Q_1(1)$ line, which is due to the fact that the $v=1$ excitation in the parahydrogen host crystal can be created in any state $\mathbf{k}$, is therefore exactly the same as that of the $Q_1(0)$ line. The frequencies corresponding to the peaks of the $Q_1(0)$ and $Q_1(0)+Q_1(1)$ infrared lines should therefore satisfy the relation

$$\nu_{IR}[Q_1(0)+Q_1(1)]=\nu_{IR}[Q_1(0)]+\nu_{IR}[Q_1(1)]. \quad (111)$$

The observed value of the left-hand side is[29] 8299.5 cm^{-1}, and that of the right-hand side is equal to[1] 415.0+4146.6=8299.6 cm^{-1}. Relation (111) is therefore very well satisfied.

9. FREQUENCY ANALYSIS OF THE ROTATION-VIBRATION TRANSITIONS AND DETERMINATION OF THE INTERMOLECULAR-COUPLING CONSTANTS

From the observed frequencies of the zero-phonon lines in the infrared and Raman spectra of solid parahydrogen information can be obtained about the magnitude of the intermolecular coupling constants using the formulas derived in the preceding sections. This is discussed in the following subsections where we consider in turn the pure rotational, the pure vibrational, the rotation–vibrational, and the overtone transitions. We also derive a number of predictions about certain frequency shifts and splittings, and finally we indicate how the adequacy and consistency of the model underlying the calculations can be tested. In our model the quadrupolar coupling constants are assumed to have the theoretical values based on the quadrupole matrix elements calculated for the free molecules.[24]

A. Crystalline-Field Constant ϵ_{2c}

According to Eq. (59), the pure rotational Raman line consists of three components corresponding, in order of increasing frequency, to $m=\pm1$, ±2, 0, and the separations in the Raman triplet are therefore given by

$$\Delta_1=\nu_R[S_0(0)]_{\pm2}-\nu_R[S_0(0)]_{\pm1} = 5(0.903\epsilon_{00}+\tfrac{1}{21}\epsilon_{4c})-\tfrac{3}{7}\epsilon_{2c}, \quad (112)$$

$$\Delta_2=\nu_R[S_0(0)]_0-\nu_R[S_0(0)]_{\pm2} = 5(0.903\epsilon_{00}+\tfrac{1}{21}\epsilon_{4c})+\tfrac{4}{7}\epsilon_{2c}.$$

The difference between the two separations is given by

$$\Delta_1-\Delta_2=-\epsilon_{2c}. \quad (113)$$

The separations Δ_1 and Δ_2 have been measured[3] to an accuracy of about 0.01 cm^{-1}. The experimental value of the left-hand side is 0.03 cm^{-1}, and therefore we get

$$\epsilon_{2c}=-(0.03\pm0.02)\text{ cm}^{-1}. \quad (114)$$

This result has been discussed previously[8] and the very small value of ϵ_{2c} has been attributed to a cancellation of the two contributions to ϵ_{2c} coming from the homogeneous deviation of the lattice from the hcp structure and from the local distortion of the lattice resulting from the coupling between the rotational motion of the molecules and the lattice vibrations. There is independent evidence[8] for the smallness of ϵ_{2c} from the temperature independence of the integrated intensity of the infrared $Q_1(1)$ line at low ortho concentrations. We therefore regard it as well established that ϵ_{2c} is less than 0.1 cm^{-1} and most likely of the order of magnitude -10^{-2} cm^{-1}.

B. Crystalline-Field Constant ϵ_{4c} and the Frequency of the $S_0(0)$ Infrared Line

From the Eqs. (112) we obtain the following relation between ϵ_{00} and ϵ_{4c}:

$$\tfrac{4}{7}\Delta_1+\tfrac{3}{7}\Delta_2=5(0.903\epsilon_{00}+\tfrac{1}{21}\epsilon_{4c}). \quad (115)$$

The experimental value of the left-hand side is[3] (2.00 ± 0.01) cm^{-1}, and we therefore get

$$0.903\epsilon_{00}+\tfrac{1}{21}\epsilon_{4c}=(0.400\pm0.002)\text{ cm}^{-1}. \quad (116)$$

We can obtain a second relation between ϵ_{00} and ϵ_{4c} by considering the infrared $S_0(0)$ line. When we define

the average frequency of the Raman $S_0(0)$ triplet as

$$\bar{\nu}_R[S_0(0)]=\tfrac{1}{5}\sum_{m=-2}^{+2}\nu_R[S_0(0)]_m, \qquad (117)$$

we get from Eqs. (59) and (60)

$$\nu_{IR}[S_0(0)]-\bar{\nu}_R[S_0(0)]=4.20\epsilon_{00}+\tfrac{1}{21}\epsilon_{4c}-\tfrac{2}{7}\epsilon_{2c}. \qquad (118)$$

The Raman frequencies are known very accurately[3] and we get $\bar{\nu}_R[S_0(0)]=(353.44\pm0.01)$ cm^{-1}. The frequency of the $S_0(0)$ infrared line has been measured by Kiss[30] and his result is $\nu_{IR}[S_0(0)]=(355.6\pm0.3)$ cm^{-1}. Using these values we obtain from Eqs. (116) and (118) the empirical value $\epsilon_{00}=(0.55\pm0.10)$ cm^{-1}, whereas the theoretical value [Eq. (57)] is given by $\epsilon_{00}=0.580$ cm^{-1}. In our opinion the theoretical value is more reliable and more accurate than the empirical one derived here, and we adopt the theoretical value of ϵ_{00}. We can then obtain from Eq. (116), i.e., from the Raman frequencies, a value of ϵ_{4c}:

$$\epsilon_{4c}=-(2.60\pm0.05)\text{ cm}^{-1}. \qquad (119)$$

As expected from the fact that ϵ_{4c} does not vanish in a perfect hcp lattice whereas ϵ_{2c} does, the constant ϵ_{4c} is much larger than ϵ_{2c}, and the value (119) does not appear to be unreasonable. When we use the result (119) in Eq. (118), we obtain the following predicted value for the frequency of the $S_0(0)$ infrared line:

$$\nu_{IR}[S_0(0)]=(355.76\pm0.01)\text{ cm}^{-1}, \qquad (120)$$

which is consistent with the measured value (355.6 ± 0.3) cm^{-1}. It is hoped that this frequency will be measured more accurately, so that a check on the value of the coupling constants ϵ_{00} and ϵ_{4c} can be obtained.

C. First Consistency Relation

To exhaust the information contained in the measured frequencies of the pure rotational lines, we consider the absolute frequency of the rotational transition in the solid. This can be done most conveniently by considering the mean Raman frequency defined by Eq. (117), which is given by [Eq. (59)]

$$\bar{\nu}_R[S_0(0)]=\nu_g[S_0(0)]-17.1\mu_1-1.3\mu_2-\epsilon_s, \qquad (121)$$

from which we obtain the relation

$$17.1\mu_1+1.3\mu_2+\epsilon_s=(1.0\pm0.1)\text{ cm}^{-1}. \qquad (I)$$

The values of the parameters μ_1, μ_2, and ϵ_s are not known theoretically with sufficient accuracy to be useful in the present context, and our aim is therefore to derive a number of relations between them which is larger than the number of unknown parameters. This enables us to test the adequacy and consistency of the model. The relations of this type are called consistency relations and they are numbered by Roman numerals.

[30] Z. J. Kiss, Ph.D. thesis, University of Toronto, 1959 (unpublished).

D. Vibrational-Coupling Constant

From Eqs. (67) and (68) we obtain the following expression for the difference between the frequencies of the infrared and Raman $Q_1(0)$ vibrational lines:

$$\nu_{IR}[Q_1(0)]-\nu_R[Q_1(0)]=6.6\epsilon'. \qquad (122)$$

The experimental value of the left-hand side is equal to[1] $4153.0-4149.8=3.2$ cm^{-1}, and we get

$$\epsilon'=(0.49\pm0.01)\text{ cm}^{-1}. \qquad (123)$$

This value is in good agreement with the value obtained from the concentration dependence of the $Q_1(0)$ and $Q_1(1)$ Raman lines.[4] The value given by Eq. (123) has been used by James and Van Kranendonk[22] to calculate the anomalous intensity ratio of the vibrational Raman lines in solid hydrogen. This ratio depends sensitively on the value of ϵ' and excellent agreement with the experimental data was obtained. The value of ϵ' derived here can therefore be regarded as well established.

E. Second and Third Consistency Relations

We can obtain a second relation between the unknown parameters from the pure vibrational lines by eliminating the constant ϵ' from Eqs. (67) and (68), giving

$$\tfrac{10}{11}\nu_{IR}[Q_1(0)]+\tfrac{1}{11}\nu_R[Q_1(0)]=\nu_g[Q_1(0)]-299.8\mu_1-170.8\mu_2. \qquad (124)$$

The left-hand side has the value $4152.7-4161.2=-(8.3\pm0.2)$ cm^{-1}, and we get

$$299.8\mu_1+170.8\mu_2=(8.3\pm0.2)\text{ cm}^{-1}. \qquad (II)$$

A third relation can be obtained by considering the $Q_1(1)$ infrared line at very low ortho concentrations. The frequency of this line is given by Eq. (72). Using the result (123) and the experimental value[1] $\nu_{IR}[Q_1(1)]=4146.6$ cm^{-1} [this line is denoted by $Q_1(0)-\delta_a$ in Ref. 1, but it is shown in Ref. 8 that this line must be identified with the $Q_1(1)$ line], we get

$$300\mu_1+171.4\mu_2=(8.6\pm0.2)\text{ cm}^{-1}, \qquad (III)$$

which is consistent with relation (II). The relations (II) and (III) cannot be used to derive values for μ_1 and μ_2.

F. Frequency of the $S_1(0)$ Infrared and Raman Transitions

The transitions to the bound $v=1, J=2$ complex give rise to a Raman triplet and a single infrared line as in the pure rotational spectrum, except that the triplet is narrower and that the levels are inverted. From

Eq. (99) it follows that the Raman active levels in the $S_1(0)$ band correspond in the order of increasing frequency to $m=0, \pm 2, \pm 1$. The separations in the $S_1(0)$ Raman triplet are hence given by

$$\Delta_1' = \nu_R[S_1(0)]_{\pm 2} - \nu_R[S_1(0)]_0 = \Delta' - \tfrac{4}{7}\epsilon_{2c},$$
$$\Delta_2' = \nu_R[S_1(0)]_{\pm 1} - \nu_R[S_1(0)]_{\pm 2} = \Delta' + \tfrac{3}{7}\epsilon_{2c}, \quad (125)$$

where $\Delta' = \frac{1}{7}(3\Delta_1' + 4\Delta_2')$ is given by

$$\Delta' = -\tfrac{5}{21}\epsilon_{4c} + \frac{15}{2}\frac{\epsilon_{01}^2}{W_1} - 44\frac{\epsilon_{01}^2\epsilon_{00}}{W_1^2} - 5S_1^+\epsilon_{00}. \quad (126)$$

S_1^+ is defined by Eq. (92) and has the value $S_1^+ = 0.059$. Using the result (119) and the known values of the quadrupolar coupling constants, we obtain

$$\Delta' = 0.62 + 0.17 - 0.03 - 0.17 = 0.59 \text{ cm}^{-1},$$
$$\Delta_1' = 0.61 \text{ cm}^{-1}, \quad (127)$$
$$\Delta_2' = 0.58 \text{ cm}^{-1}.$$

The observed $S_1(0)$ Raman line,[4] shown in Fig. 5, consists of a main maximum at a frequency of 4485.9 cm^{-1} accompanied by a satellite on the low-frequency side, separated from the main peak by $\sim$0.6 cm^{-1}. As is shown at the end of this subsection, both theoretically and experimentally the $S_1(0)$ infrared line coincides in frequency with the $m=\pm 2$ component of the Raman triplet, within the accuracy of the measurements. We must therefore identify the main maximum with the $m=\pm 2$ component and the satellite on the low-frequency side with the $m=0$ component. The calculated separation $\Delta_1' = 0.61$ cm^{-1} is in excellent agreement with the observed[4] value $\Delta_1' = (0.6 \pm 0.2)$ cm^{-1}. According to this interpretation the $m=\pm 1$ component should lie at the high-frequency side at a separation $\Delta_2' = 0.58$ cm^{-1} from the main maximum, and it would be interesting if this component could be resolved experimentally.

The main contribution to the splitting Δ_1' comes from the crystalline-field term ϵ_{4c}, viz., 0.62 cm^{-1}. The agreement between the calculated and observed value of Δ_1' therefore provides confirmation of the value of ϵ_{4c} [Eq. (119)] derived from the rotational spectrum.

The difference between the infrared line and the $m=\pm 2$ Raman component follows from Eqs. (93) and (94):

$$\nu_{IR}[S_1(0)] - \nu_R[S_1(0)]_{\pm 2} = (S_1^- - S_1^+)\epsilon_{00}. \quad (128)$$

The right-hand side has the value $(0.21-0.06)\times 0.580 = 0.09$ cm^{-1}. The experimental value of the left-hand side is equal to $(4486.0\pm 0.1) - (4485.9\pm 0.1) = (0.1\pm 0.2)$ cm^{-1}, in good agreement with the calculated value. This agreement and the fact that the other components are 0.6 cm^{-1} away form the basis of the interpretation of the Raman triplet given earlier.

Since we have exploited fully the differences between the $S_1(0)$ infrared and Raman lines, we can obtain only one additional relation from the observed absolute frequencies of the $S_1(0)$ transitions. It is most convenient to use for this purpose the $S_1(0)$ infrared line. Using the values of the parameters determined in the preceding sections, we obtain from Eq. (94) the relation

$$\nu_{IR}[S_1(0)] = \nu_g[S_1(0)] - 317.5\mu_1 - 174.8\mu_2 - \epsilon_s' - 3.60. \quad (129)$$

The experimental value of the left-hand side is[1] 4486.0 cm^{-1} and the frequency in the gas is 4497.8 cm^{-1} (cf. Table III), so that we get

$$317.5\mu_1 + 174.8\mu_2 + \epsilon_s' = (8.3\pm 0.2) \text{ cm}^{-1}, \quad \text{(IV)}$$

and this is the fourth consistency relation.

G. Mean Frequency of the Rotation-Vibration Band

We can derive a further relation from the mean frequency of the infrared absorption band corresponding to the double transitions $Q_1(0)+S_0(0)$. Equation (96) gives a formula for the mean frequency of the combined $S_1(0)$ and $Q_1(0)+S_0(0)$ bands, and an experimental value of this mean frequency can be obtained from the observed[1] absorption profile and the observed intensity ratio of these bands. The frequency of the $S_1(0)$ line is 4486.0 cm^{-1}, the mean frequency of the $Q_1(0)+S_0(0)$ band is 4507.3 cm^{-1}, and the intensity ratio of the two is 1/15, and we therefore obtain

$$\langle\nu\rangle = \tfrac{1}{16}(4486.0 + 15\times 4507.3) = 4506.0 \text{ cm}^{-1}. \quad (130)$$

Using this value for $\langle\nu\rangle$ in Eq. (101), we get the fifth consistency relation

$$316.9\mu_1 + 172.2\mu_2 + \tfrac{23}{24}\epsilon_s + \tfrac{1}{24}\epsilon_s' = (8.9\pm 0.2) \text{ cm}^{-1}. \quad \text{(V)}$$

The uncertainty in the right-hand side is difficult to estimate but is at least as large as indicated. It arises partly from the uncertainties in the observed frequencies and partly from the errors in the calculated ratio of the unperturbed intensities [Eq. (99)] and the observed ratio of the actual intensities.

H. Overtone and Double-Vibrational Transitions

In Sec. 8 we have discussed a number of overtone and double transitions. We first consider the $S_2(0)$ infrared line which has been observed by Gush.[29] In the formula (103) for the frequency of this line, the coupling constant ϵ_{00} is given by Eq. (77) and has the value $\epsilon_{00} = 0.701$ cm^{-1}, giving

$$\nu_{IR}[S_2(0)] = \nu_g[S_2(0)] - 619.9\mu_1 - 401.1\mu_2 - \epsilon_s' - 2.36. \quad (131)$$

The observed frequency in the solid is[29] (8387.4 ± 0.2) cm^{-1} and that in the gas is (8406.4 ± 0.2) cm^{-1} (cf. Table III) and we get from Eq. (131)

$$619.9\mu_1 + 401.1\mu_2 + \epsilon_s' = (16.6\pm 0.4) \text{ cm}^{-1}, \quad \text{(VI)}$$

which is the sixth consistency relation.

The other overtone and double vibrational transitions discussed in Sec. 8, such as the $S_1(0)+S_1(0)$ transition, do not give rise to further independent relations. We have already exploited the splittings in these lines, and the mean frequencies are exactly twice the frequencies of the component transitions. With the presently available experimental data the relation (VI) is therefore the last relation we can derive.

10. SUMMARY AND CONCLUSIONS

The effects of the intermolecular interaction on the rotational and vibrational levels in solid hydrogen have been analyzed by constructing a dynamical model for the H_2 molecule and by characterizing the various types of interaction operative in the solid by a number of parameters some of which are calculated theoretically and some are determined empirically. In this section we review our method of analysis, summarize the results obtained by combining our theoretical formulas with the presently available experimental data, and discuss to what extent the various theoretical predictions concerning exciton interactions and lattice self-energy effects are confirmed by the experimental data.

The dynamical model used for the H_2 molecule is the Dunham model which is obtained by expanding the intramolecular potential in powers of the vibrational coordinate (cf. Sec. 2). The model is characterized by the following six parameters: ω_e, which determines the harmonic part of the intramolecular potential; the four anharmonicity constants a_1, $\cdots$, a_4; and λ, the parameter measuring the strength of the rotation–vibration interaction. The values of these parameters are obtained from the spectroscopic data on gaseous hydrogen, i.e., from data which are independent of the spectroscopic data on the solid. The model for the intramolecular dynamics therefore does not introduce any "adjustable parameters" into our analysis, and the model can be regarded as completely given.

The intermolecular interaction relevant to the present analysis is characterized by the ten parameters μ_1, μ_2, ϵ', ϵ_{2c}, ϵ_{4c}, ϵ_0, ϵ_2, ϵ_4, ϵ_s, and ϵ_s'. The isotropic interaction acts only on the vibrational coordinates and is determined by the two parameters μ_1 and μ_2, defined by Eq. (27), and by the vibrational coupling parameter ϵ', defined by Eq. (61). The anisotropic interaction is divided into two similar parts. The first part is equal to a sum of terms each depending on the orientation of only one molecule. This crystalline-field type of interaction is determined by the parameters ϵ_{2c} and ϵ_{4c}, defined by Eq. (44). Two parameters suffice because we restrict ourselves to the rotational states $J=0, 1, 2$. The second part of the anisotropic interaction is equal to a sum over all pairs of molecules of terms which depend on the orientations of two molecules. This interaction is determined by the three parameters ϵ_0, ϵ_2, ϵ_4, defined by Eq. (51). Our basic assumption is that this rotational–coupling interaction is given entirely by the quadrupole–quadrupole interaction and that the quadrupole moments are equal to those of the isolated molecules. This means that we put the parameters ϵ_0 and ϵ_2 equal to zero and that we assume that ϵ_4 has the value corresponding to the quadrupolar interaction, which is given by Eq. (55). For the matrix elements of the quadrupole moment between the various rotation–vibration states of the molecules we take the theoretical values calculated by Karl and Poll.[24] Finally, the parameters ϵ_s and ϵ_s', defined by Eqs. (48) and (94), respectively, determine the self-energy effects in the $S_0(0)$ and $S_1(0)$ states, respectively, arising from the interaction between the rotational motion of the molecules and the lattice vibrations. Theoretical estimates[9] indicate that ϵ_s is of the order of magnitude of 1 cm^{-1} and that ϵ_s' is about a factor $\frac{1}{2}$ smaller. The empirical value of ϵ_s turns out to be about 0.5 cm^{-1}, whereas no reliable value of ϵ_s' can be obtained. Because of its expected small value we therefore put ϵ_s' equal to zero. We are then left with the six unknown parameters μ_1, μ_2, ϵ', ϵ_{2c}, ϵ_{4c}, and ϵ_s, and we now summarize the results obtained on the basis of the assumptions explained in this paragraph.

(1) The rotational $S_0(0)$ Raman triplet of pure parahydrogen, reproduced in Fig. 1, shows two separations, Δ_1 and Δ_2, which are not exactly equal. The difference $\Delta_1-\Delta_2$ depends only on the crystalline-field parameter ϵ_{2c}, cf. Eqs. (112) and (113). From the observed value of $\Delta_1-\Delta_2$ we can therefore obtain an unambiguous empirical value of this parameter: $\epsilon_{2c}=-(0.03\pm0.02)$ cm^{-1}. This result is discussed after Eq. (114).

(2) The appropriately weighted average Δ of the two separations Δ_1 and Δ_2 depends only on the quadrupolar-coupling constant ϵ_{00} and on the crystalline-field parameter ϵ_{4c} [cf. Eq. (115)]. When we assume that ϵ_{00} is equal to the theoretical value for the free molecules $\epsilon_{00}=0.580$ cm^{-1}, the observed value of $\Delta=(2.00\pm0.01)$ cm^{-1} leads to the empirical value $\epsilon_{4c}=-(2.60\pm0.05)$ cm^{-1}. This result is discussed just before and after Eq. (119).

(3) With the help of the values of the parameters ϵ_{00}, ϵ_{2c}, and ϵ_{4c} given above, we can calculate the difference between the frequency of the $S_0(0)$ infrared line and the mean frequency of the $S_0(0)$ Raman triplet [cf. Eq. (118)]. Using the observed value of the mean Raman frequency we obtain in this way the predicted value (355.76 ± 0.01) cm^{-1} for the $S_0(0)$ infrared frequency, in good agreement with the observed value[30] of (355.6 ± 0.3) cm^{-1}. A more precise measurement of this frequency would make possible the determination of an empirical value of the quadrupolar constant ϵ_{00}, and this would provide a check on our assumption that ϵ_{00} is given by the theoretical value for free molecules.

(4) So far we have used only the differences in frequency of the $S_0(0)$ lines which are independent of

the parameters μ_1, μ_2, and ϵ_s [cf. Eq. (121)]. Using the observed value of the mean Raman frequency we obtain the first consistency relation, Eq. (I), between μ_1, μ_2, and ϵ_s.

(5) We have now exhausted the information obtainable from the pure rotational spectra, and we turn to the pure vibrational spectra. The difference between the frequencies of the $Q_1(0)$ infrared and Raman lines depends only on the vibrational coupling constant ϵ' [cf. Eq. (122)] and from the observed frequencies we obtain the empirical value $\epsilon' = (0.49 \pm 0.01)$ cm^{-1}. This result is discussed after Eq. (123).

(6) The appropriately weighted average of the absolute frequencies of the infrared and Raman $Q_1(0)$ lines depends only on μ_1 and μ_2 [cf. Eq. (124)] and from the measured frequencies of these lines we obtain the second consistency relation (II). Similarly, from the observed frequency of the $Q_1(1)$ infrared line at very low orthohydrogen concentrations, we obtain another relation between μ_1 and μ_2, the third consistency relation (III). The effect of the interaction described by μ_1 and μ_2 on the $Q_1(0)$ and $Q_1(1)$ transitions is practically the same [cf. Eqs. (68) and (72)]. The fact that the relations (II) and (III) are almost identical indicates that the measurements of the $Q_1(0)$ and $Q_1(1)$ frequencies are consistent within the experimental error and also confirms the identification of the $Q_1(1)$ component of the Q branch.[8]

(7) We next turn to the $S_1(0)$ rotation–vibration transitions. The $S_1(0)$ Raman line is predicted to be a narrow triplet with separations that can be calculated with the help of the results obtained so far [cf. Eq. (127)]. Good agreement with the experimental result, shown in Fig. 5, is obtained, as discussed in more detail in Sec. 9F.

(8) The $S_1(0)$ infrared line is predicted practically to coincide in frequency with the $m = \pm 2$ component of the $S_1(0)$ Raman frequency [cf., Eq. (128)] and this result is also in agreement with the experimental data.

(9) The absolute frequency of the $S_1(0)$ transition gives a relation between μ_1, μ_2 and ϵ_s' [cf. Eq. (129)] which yields the fourth consistency relation (IV). We remark that the $S_1(0)$ infrared line, which is the sharp line in Fig. 4, is shifted by an amount -3.45 cm^{-1} due to the fact that the $J=2$ excitation in the upper state is imperfectly localized on the $v=1$ molecule. This shift is represented by the terms containing D and D' in Eq. (94). If this shift were neglected, the relation (IV) would be clearly incompatible with the other consistency relations. We can therefore say that this shift in the energy of the bound $v=1, J=2$ complex is confirmed by the experimental data. One can see this more quantitatively by determining a set of values of μ_1 and μ_2 from the consistency relations other than relation (IV) and using these values in the expression (94) for the $S_1(0)$ frequency. If the terms D and D' are neglected, a frequency is obtained which is clearly in conflict with the data, whereas if these terms are included, agreement within the experimental error is obtained.

(10) The structure of the $Q_1(0)+S_0(0)$ infrared band shown in Fig, 4 has not yet been analyzed, but we have derived a sum rule, Eq. (101), for the mean frequency of the combined $S_1(0)$ and $Q_1(0)+S_0(0)$ band. This mean frequency depends only on μ_1, μ_2, ϵ_s, and ϵ_s' and using the experimental results we get the fifth consistency relation (V).

(11) The fine structure of the $S_1(0)$ line appearing in the presence of low orthohydrogen concentrations, shown in Fig. 6, can be calculated using the known quadrupolar and crystalline field constants and taking into account the imperfect localization of the $J=2$ excitation. Good agreement with the observed fine structure is obtained. This result lends strong support to our assumption concerning the quadrupolar coupling constants, as discussed in Sec. 7D.

(12) We now turn to the overtone and double vibrational transitions. In the Eq. (103) for the frequency of the $S_2(0)$ infrared line all quantities are known except μ_1, μ_2, and ϵ_s', and from the measured frequency of this line we obtain the relation (VI).

(13) The frequency of the $Q_1(0)+Q_1(1)$ double transition at very low orthohydrogen concentrations should be equal to the sum of the $Q_1(0)$ and $Q_1(1)$ frequencies [cf. Eq. (111)] and this prediction is also verified by the experimental data.

(14) The splitting of the $S_1(0)+S_1(0)$ infrared doublet can be calculated using the quadrupolar coupling constants and taking into account the imperfect localization of the two $J=2$ excitations in the upper state [cf. Eq. (110)]. The calculated separation, 2.0 cm^{-1}, is in good agreement with the observed value (2.1 ± 0.1) cm^{-1}. The displacement of the mean frequency of the doublet due to the forces depending on μ_1 and μ_2 is exactly twice that of the $S_1(0)$ transition, and no independent consistency relation can hence be obtained from the absolute frequency of the double transition.

(15) We must finally discuss the six consistency relations (I)–(VI) between the remaining unknown parameters μ_1, μ_2, ϵ_s, and ϵ_s'. We have already remarked that ϵ_s' is expected to be considerably smaller than ϵ_s, and since moreover the relations (I)–(VI) are relatively insensitive to the value of ϵ_s', we may put $\epsilon_s' = 0$. Using rounded-off values of the coefficients of μ_1 and μ_2, we can write the consistency relations in the form

$$S_0(0): \quad 17.1\mu_1 + 1.3\mu_2 + \epsilon_s = 1.0 \pm 0.1, \qquad \text{(I)}$$

$$Q_1(0): \quad 300\mu_1 + 171\mu_2 = 8.3 \pm 0.2, \qquad \text{(II)}$$

$$Q_1(1): \quad 300\mu_1 + 171\mu_2 = 8.6 \pm 0.2, \qquad \text{(III)}$$

$$S_1(0): \quad 318\mu_1 + 175\mu_2 = 8.3 \pm 0.2, \qquad \text{(IV)}$$

$$Q_1(0)+S_0(0): \quad 317\mu_1 + 172\mu_2 + \epsilon_s = 8.9 \pm 0.2, \qquad \text{(V)}$$

$$S_2(0): \quad 310\mu_1 + 201\mu_2 = 8.3 \pm 0.2. \qquad \text{(VI)}$$

The symbols in front of the equations indicate the spectral features from which the relations have been obtained. It is evident that the relations (II) and (III) are compatible within the given accuracy. We shall replace these relations by the single relation

$$Q_1: \quad 300\mu_1+171\mu_2=8.4\pm0.2. \qquad \text{(II')}$$

Theoretical estimates indicate that the self-energy ϵ_s, which is necessarily positive, is at most of the order of 1 cm^{-1}. From relations (IV) and (V) it is evident that ϵ_s is indeed positive and approximately equal to (0.5 ± 0.3) cm^{-1}. A more accurate estimate of ϵ_s can be obtained from (I) as follows. If ϵ_s did not appear, we could test the consistency of the relations (I)–(VI) by plotting the straight lines corresponding to these equations in the μ_1, μ_2 plane and seeing whether or not these lines pass approximately through one point. For $\epsilon_s \neq 0$, we can draw the lines in the μ_1, μ_2 plane for a number of given values of ϵ_s, and this has been done in Fig. 8 for the values $\epsilon_s=0.4$, 0.5 and 0.6 cm^{-1}. The line corresponding to (V) is practically the same for these three values of ϵ_s, and indistinguishable from (IV), and for the given range of values of ϵ_s we may therefore replace (IV) and (V) by the single relation

$$318\mu_1+174\mu_2=8.4\pm0.2. \qquad \text{(IV')}$$

The uncertainties given in the right-hand members of the consistency relations correspond to a thickness of the lines in Fig. 8, which is indicated approximately by the shaded area around the line (IV'). It is clear from Fig. 8 that, within the given uncertainty, the relations (I), (II'), (IV'), and (VI) are consistent and that the best value of ϵ_s is equal to $\epsilon_s=(0.5\pm0.1)$ cm^{-1}. There is a considerable spread in the choice of μ_1 and μ_2, but a possible set of values is given by $\mu_1=3.0\times10^{-2}$ and $\mu_2=-5\times10^{-3}$. We thus arrive at the conclusion that the model on which the analysis presented in this paper is based gives an adequate description of all the Raman and zero-phonon infrared features of solid parahydrogen and ortho–para mixtures at low orthohydrogen concentrations.

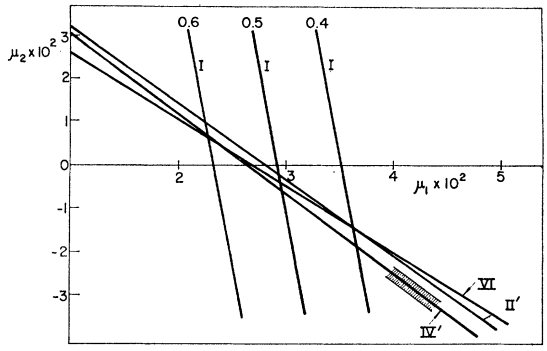

FIG. 8. Graphical representation of the consistency relations I, II', IV', and VI, between the parameters μ_1 and μ_2 characterizing the isotropic intermolecular interaction, and the rotational-phonon self-energy parameters ϵ_s and ϵ_s', for $\epsilon_s'=0$ and $\epsilon_s=0.4$, 0.5, and 0.6 cm^{-1}. Only relation I is noticeably dependent on ϵ_s. The shaded area indicates the uncertainty in the positions of the lines arising from the uncertainties in the measured frequencies. The lines should go through one point. It is evident that the best value is $\epsilon_s=0.5$ cm^{-1} and that satisfactory consistency is obtained for this value of ϵ_s but not for $\epsilon_s=0$.